JPET Fast Forward. Published on May 25, 2006 as DOI:10.1124/jpet.106.105247

JPET #105247

Anti-tumor activity of plant cannabinoids with emphasis on the effect of cannabidiol on human breast carcinoma

Alessia Ligresti, Aniello Schiano Moriello, Katarzyna Starowicz, Isabel Matias, Simona Pisanti, Luciano De Petrocellis, Chiara Laezza, Giuseppe Portella, Maurizio Bifulco and Vincenzo Di Marzo*

Endocannabinoid Research Group, Istituto di Chimica Biomolecolare, CNR Pozzuoli, Italy (AL, ASM, KS, IM, VDM); Istituto di Cibernetica, CNR Pozzuoli, Italy (ASM, LDP); Dipartimento di Biologia e Patologia Cellulare e Molecolare "L.Califano", Università di Napoli "Federico II"(SP, CL, GP, MB) and Dipartimento di Scienze Farmaceutiche, Università degli Studi di Salerno, Fisciano, Italy (SP, MB)

Running Title: Cannabidiol in cancer

***Corresponding Author:** Vincenzo Di Marzo; Istituto di Chimica Biomolecolare, CNR; Via Campi Flegrei 34; 80078 Pozzuoli, Napoli (Italy); Telephone number: 0039-081-8675093; Fax number: 0039-081-8041770; E-mail: vdimarzo@icmib.na.cnr.it

Number of text pages: 36

Number of Tables: 4

Number of Figures: 10

Number of references: 40

Number of words in Abstract: 246

Number of words in Introduction: 682

Number of words in Discussion: 1482

Abbreviations: CB_1, cannabinoid receptor type-1; CB_2, cannabinoid receptor type-2; GAPDH, glyceraldehyde-3-phosphate dehydrogenase; HMEpC, human mammary epithelial; I-RTX, 5'-iodo-resiniferatoxin; THC, Δ^9-tetrahydrocannabinol; PCR, polymerase chain reaction; RBL-2H3, rat basophilic leukemia; ROS, reactive oxygen species; TRPV1, transient receptor potential vanilloid type-1

Abstract

Δ^9-tetrahydrocannabinol (THC) exhibits anti-tumor effects on various cancer cell types, but its use in chemotherapy is limited by its psychotropic activity. We investigated the anti-tumor activities of other plant cannabinoids, i.e. cannabidiol, cannabigerol, cannabichromene, cannabidiol-acid and THC-acid, and assessed whether there is any advantage in using *Cannabis* extracts (enriched in either cannabidiol or THC) over pure cannabinoids. Results obtained in a panel of tumor cell lines clearly indicate that, of the five natural compounds tested, cannabidiol is the most potent inhibitor of cancer cell growth (IC_{50} between 6.0 and 10.6 μM), with significantly lower potency in non-cancer cells. The cannabidiol-rich extract was equipotent to cannabidiol, whereas cannabigerol and cannabichromene followed in the rank of potency. Both cannabidiol and the cannabidiol-rich extract inhibited the growth of xenograft tumors obtained by subcutaneous injection into athymic mice of human MDA-MB-231 breast carcinoma or rat v-K-*ras*-transformed thyroid epithelial cells, and reduced lung metastases deriving from intra-paw injection of MDA-MB-231 cells. Judging from several experiments on its possible cellular and molecular mechanisms of action, we propose that cannabidiol lacks a unique mode of action in the cell lines investigated. At least for MDA-MB-231 cells, however, our experiments indicate that cannabidiol effect is due to its capability of inducing apoptosis via: 1) direct or indirect activation of cannabinoid CB_2 and vanilloid TRPV1 receptors; and 2) cannabinoid/vanilloid receptor-independent elevation of intracellular Ca^{2+} and reactive oxygen species. Our data support the further testing of cannabidiol and cannabidiol-rich extracts for the potential treatment of cancer.

Introduction

The therapeutic properties of the hemp plant, *Cannabis sativa* have been known since antiquity but the recreational use of its euphoric and other psychoactive effects has restricted for a long time research on its possible pharmaceutical application. The isolation of Δ^9–tetrahydrocannabinol (THC), the main psychoactive component of *Cannabis* (Gaoni and Mechoulam, 1964), opened the way to further investigations. After the discovery of the two specific receptor types for THC, CB_1 and CB_2 (see Pertwee, 1997, for review), it became clear that most of the effects of marijuana in the brain and peripheral tissues were due to activation of these two G-protein-coupled cannabinoid receptors. However, evidence is also accumulating that some pharmacological effects of marijuana are due to *Cannabis* components different from THC. Indeed, *Cannabis sativa* contains at least 400 chemical components of which 66 have been identified to belong to the class of the cannabinoids (Pertwee, 1997).

To date, cannabinoids have been successfully used in the treatment of nausea and vomiting (see Robson 2005 for review), two common side effects that accompany chemotherapy in cancer patients. Nevertheless, the use of cannabinoids as palliatives in oncology might be somehow underestimated since increasing evidence exist that plant, synthetic and endogenous cannabinoids (endocannabinoids) are able to exert a growth-inhibitory action on various cancer cell types. However, the precise pathways through which these molecules produce an anti-tumor effect has not been yet fully characterized, also because their mechanism of action appears to be dependent on the type of tumor cell under study. It has been reported that cannabinoids can act through different cellular mechanisms, e.g. by inducing apoptosis, cell-cycle arrest or cell growth inhibition, but also by targeting angiogenesis and cell migration (see Bifulco and Di Marzo, 2002; Guzman, 2003; Kogan, 2005; for reviews). Furthermore, the anti-tumoral effects of plant, synthetic and endocannabinoids can be mediated by activation of either CB_1 (Melck et al., 2000; Bifulco et al. 2001, Mimeault et al. 2003, Ligresti et al. 2003) or CB_2 receptors, or both (Casanova et al. 2003, Sanchez et al. 2001, McKallip et al. 2005), and, at least in the case of the endocannabinoid

anandamide, by transient receptor potential vanilloid type-1 (TRPV1) receptors (Maccarrone et al., 2000; Jacobsson et al., 2001; Contassot et al., 2004) as well as by non-cannabinoid, non-vanilloid receptors (Ruiz et al., 1999). Additionally, cannabidiol has been suggested to inhibit glioma cell growth in vitro and in vivo independently from cannabinoid and vanilloid receptors (Massi et al., 2004; Vaccani et al. 2005).

The main limitation of the possible future use of THC in oncology might be represented by adverse effects principally at the level of the central nervous system, consisting mostly of perceptual abnormalities, occasionally hallucinations, dysphoria, abnormal thinking, depersonalization and somnolence (Walsh et al., 2003). However, most non-THC plant cannabinoids seem to be devoid of direct psychotropic proprieties. In particular, it has been ascertained that cannabidiol is non-psychotropic (see Mechoulam et al., 2002; Pertwee, 2004 for reviews) and may even mitigate THC psychoactivity by blocking its conversion to the more psychoactive 11-hydroxy-THC (Bornheim and Grillo, 1998; Russo and Guy, 2006). Moreover, it has been recently found that systematic variations in its constituents (i.e. cannabidiol and cannabichromene) does not affect the behavioral or neurophysiological responses to marijuana (Ilan et al., 2005). Finally, it has been also shown that, unlike THC, systemic administration to rats of cannabigerol does not provoke poly-spike discharges in the cortical electroencephalogram during wakefulness and behavioral depression (Colasanti, 1990). These and other observations reinforce the concept that at least cannabidiol, cannabigerol and cannabichromene lack psychotropic activity, and indicate that for a promising medical profile in cancer therapy, research should focus on these compounds, which instead have been poorly studied with regard to their potential anti-tumor effects. By keeping this goal in mind, we decided to investigate the anti-tumor properties of cannabidiol, cannabigerol and cannabichromene. We also screened THC-acid and cannabidiol-acid and two distinct *Cannabis* extracts (enriched in either cannabidiol or THC), where the presence of non-psychotropic cannabinoids along with THC has been reported to mitigate the potential side effects of the latter compound in clinical trials (Russo and Guy, 2006).

Methods

Drugs. All plant cannabinoids, the two cannabinoid acids and the two *Cannabis* extracts were kindly provided by GW-Pharmaceuticals (Fig. 1). Cannabidiol-rich and THC-rich extracts contained approximately 70% of cannabidiol or THC, respectively, together with lesser amounts of other cannabinoids. The two cannabinoid receptor antagonists, N-(piperidin-1-yl)-5-(4-chlorophenyl)-1-(2,4-dichlorophenyl)-4-methyl-1H-pyrazole-3-carboxamide HCl [SR141716A] and N-[(1S)-endo-1,3,3-trimethylbicyclo[2.2.1]heptan-2-yl]-5-(4-chloro-3-methylphenyl)-1-(4-methylbenzyl)-1-pyrazole-3-carboxamide (SR144528), were a kind gift from Sanofi-Aventis, whereas methyl-beta-cyclodextrin, all the anti-oxidant drugs (α-tocopherol, Vitamin C, Astaxantine), *N*-Acetyl-Asp-Glu-Val-Asp-aldehyde (Ac-DEVD-CHO) and BAPTA-M were purchased from Sigma-Aldrich (St. Louis, MO). The endocannabinoid uptake inhibitor (*S*)-1'-(4-hydroxybenzyl)-*N*-ethyl-oleoylamide [OMDM-2] was synthesized as previously described in Ortar et al., 2003. Finally all the TRPV1 or cannabinoid receptor agonists and antagonists (capsaicin, resiniferatoxin, arachidonoyl-2-chloro-ethylamide, 1,1-dimethylbutyl-1-deoxy-Δ^9-tetrahydrocannabinol [JWH-133], N-(piperidin-1-yl)-5-(4-iodophenyl)-1-(2,4-dichlorophenyl)-4-methyl-1H-pyrazole-3-carboxamide [AM251], 6-iodo-2-methyl-1-[2-(4-morpholinyl)-ethyl]-1H-indol-3-yl](4-methoxyphenyl)-methanone [AM-630]) were obtained from Tocris Cookson (Bristol, United Kingdom).

Cell cultures. Cell lines from various origins (MCF-7 and MDA-MB-231 human breast carcinoma cells, DU-145 human prostate carcinoma cells, CaCo-2 human colorectal carcinoma cells, AGS human gastric adenocarcinoma cells, C_6 rat glioma cells, KiMol rat thyroid cells transformed with the v-K-*ras* oncogene and RBL-2H3 rat basophilic leukaemia cells) were maintained at 37°C in a humidified atmosphere containing 5% of CO_2. Media, sera and subculturing procedures differed from line to line and were according to the information provided in each case by the supplier company (DSMZ, Braunschweig, Germany). Primary cells derived from normal human mammary

glands were purchased by Cell Applications, Inc. (San Diego, CA) and cultured as described in the data sheet from the supplier.

Cell proliferation assay. Six-well culture plates were incubated at 37°C at a cell density of $5x10^4$cells/well in a humidified atmosphere containing 5% of CO_2. Three hours after seeding, vehicle or cannabinoids at different concentrations were added to the medium and then daily with each change of medium for 4 days and the effect of compounds on cell growth was measured by Crystal Violet vital staining. After staining, cells were lysated in 0.01% of Acetic Acid and analyzed by spectrophotometer analysis (Perkin Elmer Lambda 12, λ=595nm). OD values from vehicle-treated cells were considered as 100% of proliferation. Statistical analysis was performed using ANOVA followed by Bonferroni test.

Detection of reactive oxygen species (ROS). Intracellular ROS generation was determined by spectrofluorimetric analysis. MDA-MB-231 cells were plated ($16x10^3$cells/well) in Porvair PS-White Microplate 96 well (Perkin-Elmer) for 12 hours. The day of the experiment, cells were rinsed once with Tyrode's buffer, then loaded (1 hour at 37°C in darkness) with 10 μM of 2',7'-dichlorofluorescin diacetate (H_2DCFDA fluorescent probe, Molecular Probes) in presence of 0.05% Pluronic. ROS-induced fluorescence of intracellular H_2DCFDA was measured with a microplate reader (Perkin Elmer LS50B, λ_{Ex} 495nm - λ_{Em} 521nm). Fluorescence detections were carried out after the incubation of 100 μM H_2O_2 and/or increasing concentrations of cannabidiol at room temperature in the darkness for different times (0-30-60-120 minutes). The fluorescence measured at time zero was considered as basal ROS production and subtracted from the fluorescence at different times (Δ_1). Data are reported as mean ± SE of Δ_2, i.e. fluorescence Δ_1 values at different doses subtracted of the Δ_1 values of cells incubated with vehicle. In some experiments a buffer containing $MgCl_2$ in amounts equivalent to $CaCl_2$ and EGTA 0.1 mM, and cells pre-loaded for 30 min with BAPTA-M (40 μM), were used instead.

RT-PCR analysis. Total RNAs from these cells were extracted using the Trizol reagent according to the manufacturer's recommendations (GibcoBRL). Following extraction, RNA was precipitated using ice-cold isopropanol, resuspended in diethyl pyrocarbonate (Sigma)-treated water and its integrity was verified following separation by electrophoresis on a 1% agarose gel containing ethidium bromide. RNA was further treated with RNAse-free DNAse I (Ambion DNA-free™ kit) according the manufacturer's recommendations to digest contaminating genomic DNA and to subsequently remove the DNAse and divalent cations.

The expression of mRNAs for CB_1, CB_2, TRPV1 and GAPDH were examined by semiquantitative reverse transcription coupled to the polymerase chain reaction (RT-PCR). Total RNA was reverse-transcribed using random primers. DNA amplifications were carried out in PCR buffer (Invitrogen) containing 2μl of cDNA, 500 μM dNTP, 2 mM MgCl2, 0.8 μM of each primer and 0.5 U Taq polymerase platinium (Invitrogen). The thermal reaction profile consisted of a denaturation step at 94°C for 1 min, annealing 55°C (GAPDH) or 57°C (CB_2 and TRPV1) or 60°C (CB_1) for 1 min and an extension step at 72°C for 1 min. A final extension step of 10 min was carried out at 72°C. The PCR cycles observed to be optimal and in the linear portion of the amplification curve were 24 for GAPDH, 29 for CB_1 and CB_2, and 28 for TRPV1 (data not shown). Reaction was performed in a PE Gene Amp PCR System 9600 (Perkin Emer). After reaction, the PCR products were electrophoresed on a 2% agarose gel containing ethidium bromide for UV visualization.

Specific rat and human oligonucleotides were synthesized on the basis of cloned rat and human cDNA sequences of CB_1 (Genbank accession numbers: NM_012784.3 and X81120 for rat and human respectively), CB_2 (Genbank accession numbers: NM_0205433 and X74328 for rat and human respectively), TRPV1 (Genbank accession numbers: NM_031982 and NM_080706.2 for rat and human respectively) and GAPDH (Genbank accession numbers: NM_017008.2 and BT006893.1 for rat and human respectively).

For rat and human CB_1, the primers sequences were 5'- GAT GTC TTT GGG AAG ATG AAC AAG C -3' (nt 1250-1274 for rat and nt 1187-1211 for human; sense) and 5'- AGA CGT GTC TGT GGA CAC AGA CAT GG -3' (nt 1558-1534 for rat and nt 1495-1470 for human; antisense). The rat CB_2 sense and antisense primers were 5'- TA(C/T) CC(G/A) CCT (A/T)CC TAC AAA GCT C -3' (nt 407-428) and 5'- C (A/T)GG CAC CTG CCT GTC CTG GTG -3' (nt 698-676), respectively. For human CB_2, the primers sequences were 5'- TTT CCC ACT GAT CCC CAA TG -3' (nt 672-691; sense) and 5'- AGT TGA TGA GGC ACA GCA -3' (nt 1000-983; antisense). For rat TRPV1, the primers sequences were 5'- GAC ATG CCA CCC AGC AGG -3' (nt 2491-2508; sense) and 5'- TCA ATT CCC ACA CAC CTC CC -3' (nt 2752-2733; antisense). The human TRPV1 sense and antisense primers were 5'- TGG ACG AGG TGA ACT GGA C -3' (nt 2761-2779) and 5'- ACT CTT GAA GAC CTC AGC GTC -3' (nt 3023-3003), respectively. For rat and human GAPDH, the primers sequences were 5'- CCC TTC ATT GAC CTC AAC TAC ATG GT -3' (nt 949-974 for rat and nt 106-131 for human; sense) and 5'- GAG GGG CCA TCC ACA GTC TTC TG -3' (nt 1418-1396 for rat and nt 575-553 for human; antisense).

The expected sizes of the amplicons were 309 bp for rat and human CB_1, 291 bp for rat CB_2, 329 bp for human CB_2, 263 bp for rat TRPV1, 262 bp for human TRPV1 and 470 bp for rat and human GAPDH. In the presence of contaminant genomic DNA, the expected size of the amplicons would be 1062 bp for GAPDH (data not shown). No PCR product was detected when the reverse transcriptase step was omitted.

Western immunoblotting analysis for caspase-3. Immunoblotting analysis was performed on the cytosolic fraction of cells treated as described above, and according to previous published work (Iuvone et al., 2004). Cytosolic fraction proteins were mixed with gel loading buffer (50 mM Tris/10% SDS/10 % glycerol 2-mercaptoethanol/ 2mg bromophenol per ml) in a ratio of 1:1, boiled for 5 min and centrifuged at 10,000 x g for 10 min. Protein concentration was determined and equivalent amounts (50 µg) of each sample were separated under reducing conditions in 12% SDS-polyacrylamide minigel. The proteins were transferred onto nitrocellulose membrane, according to

the manufacturer's instructions (BioRad, Hercules, CA). The membranes were blocked by incubation at 4°C overnight in high salt buffer (50 mM Trizma base, 500 mM NaCl, 0.05% Tween-20) containing 5% bovine serum albumin and then incubated for 2 hours with anti-caspase 3 (1:2000, v:v) at room temperature, followed by incubation for 2 hours with HRP-conjugate secondary antibody (Dako, Glostrup, Denmark). The immune complexes were developed using enhanced chemiluminescence detection reagents (Amersham, United Kingdom) according to the manufacturer's instructions and exposed to Kodak X-Omat film. The bands of tau protein on X-ray film were scanned and densitometrically analyzed with a GS-700 imaging densitometer.

Immunofluorescence. For immunoreaction, MDA-MB-231 cells were seeded on sterile coverslips (22 x 22 mm, Menzel, Germany) in 6-well culture plates and incubated under standard conditions until they were at least 70 % confluent. Cultured cells were processed for immunofluorescence. After three washes with PBS, cells were fixed by incubating them in 4% (v/v) paraformaldehyde in PBS for 20 min at room temperature, rinsed with PBS, permeabilized for 15 min in 0.5% Triton X-100 in PBS and incubated overnight at 4°C with rabbit polyclonal rabbit anti-CB_1 or anti-CB_2 antibody (Cayman Chemicals, USA), both diluted 1:50 in 0.5% Triton X-100 in PBS, or goat anti-TRPV1 antibody (SantaCruz, USA) diluted 1:100 in 0.5% Triton X-100 in PBS. After three washes in PBS, fluorescence was revealed by incubation for 2 hours in a AlexaFluor488® labeled secondary anti-rabbit antibody (Molecular Probes, Invitrogen) diluted 1:100 in 0.5% Triton X-100 in PBS or AlexaFluor546® labeled secondary anti-goat antibody (Molecular Probes, Invitrogen) diluted 1:200 in 0.5% Triton X-100 in PBS. The pre-absorption of antibodies with the respective blocking peptides as well as omission of primary antibodies (control immunoreaction) resulted in much weaker or negative staining, respectively. Sections processed for immunofluorescence were studied with an epifluorescence microscope equipped with the appropriate filter (Leica DM IRB). Images were acquired using a digital Leica DFC 320 camera connected to the microscope and the image analysis software Leica IM500. Images were processed in Adobe Photoshop, with brightness and contrast being the only adjustments made.

In vivo studies: effect on xenograft models of carcinoma. All the experiments were performed by using Charles-River 6-week-old male athymic mice as described previously (Bifulco et al., 2001). Two different mouse xenograft models of tumor growth were induced by subcutaneous injection ($5x10^5$ cells) of two distinct highly invasive tumoral cell lines (KiMol or MBA-MD-231 cells) into the dorsal right side of athymic mice. Starting from the appearance of tumoral mass, pure compounds or *Cannabis* extracts were injected intra-tumor in the same inoculation region twice per week for 20 days (KiMol cells-induced tumors) or 16 days (MBA-MD-231 cells-induced tumors). THC and cannabidiol were administered at the dose of 5 mg/kg while THC-rich and cannabidiol-rich were administrated at the dose of 6.5 mg/kg, which contains 5 mg/kg of THC and cannabidiol, respectively. Tumor diameters were measured with calipers every other day until the animals were killed. Tumor volumes (V) were calculated by the formula of rotational ellipsoid (V= AxB2/2; A=axial diameter, B=rotational diameter). Results were reported as means ± SE. Statistical analysis was performed using ANOVA followed by the Bonferroni's test.

In vivo analysis: effect on experimental lung metastasis. Monocellular suspension of MDA-MB-231 cells containing 2.5×10^5 cells was injected into the left paw of 30-day-old BalB/c male mice. Animals were divided into three groups: Vehicle (n=11), cannabidiol (5 mg/kg/dose, n=14) or cannabidiol-rich (6.5 mg/kg/dose, n=14). The drugs were injected i.p. every 72 hours. Experimental metastases were evaluated 21 days after the injection. To contrast lung nodules, lungs were fixed in Bouin's fluid, and metastatic nodes were scored on dissected lung under a stereoscopic microscope. All animal studies were conducted in accordance with the Italian regulation for the welfare of animals in experimental neoplasia. All data were presented as means ± SD. Statistical analysis was performed using one-way ANOVA.

Cell cycle and apoptosis detection. Different cell lines were exposed to 10 μM of cannabidiol or cannabigerol for 48 hours at 37°C in a humidified atmosphere containing 5% of CO_2. The distribution of cells among the different phases of the cell cycle and apoptosis rate were evaluated by flow cytometric analysis of the DNA content. Cells ($5x\ 10^5$) were collected, washed twice with

PBS, fixed by ethanol 70% and kept at -20 ^{0}C for at least 4 hours. Propidium iodide (10 μg/ml) in PBS containing 100 U/ml DNAse-free RNAse was added to the cells for 15 min at room temperature. Cells were acquired by a FACSalibur flow cytometer (BD Biosciences, San Jose, CA) and then analysis was performed using ModFit LT v3.0 from Verity Software House, Inc. (Topsham, ME); 10,000 events were collected, corrected for debris and aggregate populations.

Anandamide cellular re-uptake and intracellular hydrolysis. The effect of compounds on anandamide cellular re-uptake was analyzed on rat basophilic leukemia (RBL-2H3) cells or MDA-MB-231 cells by using 2.5 μM (10,000 cpm) of [^{14}C]anandamide as described previously (De Petrocellis et al., 2000). Briefly, cells were incubated with [^{14}C]anandamide for 5 min at 37°C, in the presence or absence of varying concentrations of the compounds. Residual [^{14}C]anandamide in the incubation medium after extraction with $CHCl_3$/CH_3OH 2:1 (by volume), determined by scintillation counting of the lyophilized organic phase, was used as a measure of the anandamide that was taken up by cells (De Petrocellis et al., 2000). Non-specific binding of [^{14}C]anandamide to cells and plastic dishes was determined in the presence of 100 μM anandamide and was never higher than 30%. Data are expressed as the concentration exerting 50% inhibition of anandamide uptake (IC_{50}) calculated by GraphPad software. The effect of compounds on the enzymatic hydrolysis of anandamide was studied using membranes prepared from N18TG2 cells, incubated with the test compounds and [^{14}C]anandamide (20,000cpm; 5 μM) in 50 mM Tris-HCl, pH 9, for 30 min at 37°C. [^{14}C]Ethanolamine produced from [^{14}C]anandamide hydrolysis was measured by scintillation counting of the aqueous phase after extraction of the incubation mixture with 2 volumes of $CHCl_3$/CH_3OH 1:1 (by volume). Data are expressed as the concentration exerting 50% inhibition of [^{14}C]anandamide hydrolysis (IC_{50}), calculated by GraphPad software.

Activity at human recombinant TRPV1. The effect of the substances on $[Ca^{2+}]_i$ was determined by using Fluo-3 (Molecular Probes, Eugene, OR), a selective intracellular fluorescent probe for Ca^{2+} (De Petrocellis et al., 2000). Human embryonic kidney (HEK) 293 cells stably over-expressing human TRPV1 receptor or MDA-MB-231 cells were transferred into six-well dishes coated with

poly-L-lysine (Sigma-Aldrich, St.Luis, MO) one day prior to experiments and grown in the culture medium mentioned above. On the day of the experiment, the cells (50-60,000 cells/well) were loaded for 2 hours at 25°C with 4 μM Flu-3-methylester (Fluo3-AM, Invitrogen, Eugene, Oregon) in dimethyl sulfoxide containing 0.04% Pluoronic F-127 (Invitrogen, Eugene, Oregon). After loading, cells were washed with Tyrode's solution, pH 7.4, trypsinized, resuspended in Tyrode's solution, and transferred to the cuvette of the fluorescence detector (PerkinElmer LS50B) under continuous stirring. Experiments were carried out by measuring cell fluorescence at 25°C (λ_{EX} = 488 nm, λ_{EM} = 540 nm) before and after the addition of the test compounds at various concentrations. Data are expressed as the concentration exerting a half-maximal effect (EC_{50}). The efficacy of the effect was determined by comparing it to the analogous effect observed with 4 μM Ionomycin. In some experiments with MDA-MB-231 cells, the effect of cannabidiol was measured also in the absence of extracellular Ca^{2+} (i.e. in a Tyrode's solution containing Mg^{2+} instead of Ca^{2+}, and 0.1 mM EGTA) and in cells pre-loaded with BAPTA-M (20 μM).

Results

Effect on cancer cell growth: in vitro studies. For in vitro studies, the cannabinoids under investigation were screened for their ability to reduce cell proliferation on a collection of tumoral cell lines. cannabidiol always exhibited the highest potency with IC_{50} values ranging between 6.0 ± 3.0 μM and 10.6 ± 1.8 μM (Table 1). Cannabidiol-acid was the least potent compound. Among the other plant cannabinoids, cannabigerol was almost always the second most potent compound followed by cannabichromene (Table 1). The effect of the two *Cannabis* extracts (enriched in cannabidiol or THC) was next investigated and in some circumstances the cannabidiol-rich extract appeared slightly more potent than pure cannabidiol (Table 1). In the case of MCF-7 cells both compounds exhibited quite similar potency, as indicated by the IC_{50} values of 8.2 ± 0.3μM and 6.0 ± 1.0 μM respectively for cannabidiol and cannabidiol-rich extract (Fig. 2A), on the contrary, in the case of C_6 glioma cells, cannabidiol-rich extract also exhibited significantly higher potency than pure cannabidiol (IC_{50} 4.7 ± 0.6 μM and 8.5 ± 0.8 μM respectively, $p<0.05$, Fig. 2B). Only in the case of human DU-145 prostate carcinoma cells, plant cannabinoids induced a stimulatory effect on cancer growth at the lowest doses tested and an inhibitory effect only at the highest concentration tested (25 μM) (as also found by Sanchez et al., 2003 in another prostate carcinoma cell line). In this case, however, the cannabidiol-rich extract lacked the pro-proliferative effect even at the lowest concentration tested of 2 μM (Fig. 2C-2D).

For a comparison, we also tested cisplatinum on some cell lines, and found that this widely used anti-cancer compound as compared to cannabidiol was only 2.5-, 8.8- and 3.9-fold more potent in MCF-7, MDA-MB-231 and AGS cells (IC_{50}= 3.2 ± 0.3, 1.2 ± 0.2 and 1.9 ± 0.2 μM, respectively), and 17- and 33.6-fold more potent in C_6 and DU-145 cells (IC_{50}= 0.5 ± 0.1 and 0.6 ± 0.2 μM, respectively).

The Trypan Blue dye-exclusion method on the entire range of cells was used to detect cytotoxicity and to assess cell viability. All the compounds under investigation showed a statistically significant cytotoxic effect starting only from the highest concentration tested (25 μM) (data not shown).

Finally, to investigate the selectivity of cannabidiol effect in tumoral *vs.* non-tumoral cells, various concentrations (from 1 to 100μM) of cannabidiol on different stabilized non-tumor cell lines such as HaCat (human keratinocyte), 3T3-F442A (rat pre-adipocytes), RAW 264.7 (mouse monocyte-macrophages) were also tested. cannabidiol, at a dose similar to its IC_{50} values in the various tumoral cell lines, did not affect the vitality of non-tumor cell lines (Fig. 2E). Only at a concentration of 25 μM, which exerts nearly 100% inhibition of cancer cell growth, cannabidiol exhibited a cytotoxic effect in these non-tumoral cell lines (Fig. 2E). Lastly, it was examined the selectivity of cannabidiol *vs.* a primary cell line derived from mammary glands (Human Mammary Epithelial Cells, HMEpC) since several experiments on the mechanism of action of cannabidiol were performed using a human breast carcinoma cell line (MBA-MD-231 cells). cannabidiol affected significantly the vitality of this cell line only at a 25 μM concentration (Fig. 2F).

Effect on cancer cell growth: in vivo studies. For the in vivo studies, the efficacy of cannabidiol and its enriched extract at reducing tumor size and volume was evaluated. Mice treated with either pure cannabidiol or the cannabidiol-rich extract exhibited significantly smaller tumors in comparison with control mice. A strong and statistically significant anti-tumor effect was observed with both treatments and with both in vivo xenograft tumor models used (Fig. 3A, B). The effect of cannabidiol and cannabidiol-rich compounds on the formation of lung metastatic nodules of MBA-MD-231 cells injected into the paw was also investigated. Both cannabidiol and cannabidiol-rich, exhibited a strong and significant reduction of metastatic lung infiltration (Fig. 3C).

Study on the cellular mechanism of action of cannabidiol. With the intention of evaluate if the inhibitory effect on cell growth of cannabidiol was associated with apoptotic events or blockade of

mitogenesis, the percentage of G_1 population cells was estimated by flow cytometry. In MCF-7 cells, a hormone-sensitive cell line, cannabidiol exerted anti-proliferative effect by causing a cell cycle block at the G_1/S phase transition (Fig. 4A, Table 2). A similar result was observed in another hormone-sensitive cell line KiMol cells, where, however, the anti-proliferative effect of cannabidiol was also accompanied by a pro-apoptotic action (Fig. 4C, Table 2). Finally, in C_6 glioma and MDA-MB-231 cells (two non-hormone-sensitive cell lines) cannabidiol provoked a pure pro-apoptotic effect (Fig. 4D, Table 2). The pro-apoptotic effect of cannabidiol on MDA-MB-231 cells was also established by evaluating the involvement of caspase-3. The pro-apoptotic effect of cannabidiol was confirmed in this cell line, but not in DU-145 cells, as indicated by the pro-caspase-3 cleavage into caspase-3 by Western immunoblotting analysis following a 48 hours treatment of cells with the compound (Fig. 4E). In agreement with a role of apoptosis and caspase-3 in cannabidiol anti-cancer effect in MDA-MB-231 cells, Ac-DEVD-CHO (10 μM), an inhibitor of caspase-3, significantly attenuated the growth-inhibitory effect of both 5 and 10 μM cannabidiol as indicated by the reduction of the % inhibition of cell proliferation induced by these two doses of the cannabinoid (from 21.8 ± 3.1 to 7.8 ± 1.1% at 5 μM and from 55.8± 4.9 to 11.9± 1.6% at 10 μM; means ± SE; n=3, $p<0.01$).

Study on the molecular mechanism of action of CBD. When using PCR, we found that both vanilloid TRPV1 receptors and cannabinoid CB_1 and CB_2 receptors are expressed in most of the cell lines used in this study (Table 3). In order to estimate the involvement of TRPV1 receptors in the anti-proliferative properties, all cannabinoids were screened for their capability to generate TRPV1-mediated intracellular calcium elevation in stably transfected TRPV1-HEK293 cells. Apart from cannabidiol, only cannabigerol and cannabidiol-acid activated TRPV1 receptors, with a significantly lower potency than cannabidiol, whereas cannabichromene, THC and THC-acid were almost inactive (Fig. 5). The cannabidiol-rich extract was as efficacious and potent as cannabidiol,

whereas the THC-rich extract was more efficacious and potent than THC, possibly due to the presence of other TRPV1-active cannabinoids, including cannabidiol and cannabigerol (Fig. 5).

In order to assess whether plant cannabinoids, which are very weak agonists of CB_1 and CB_2 receptors, activate these receptors indirectly, i.e. by elevating endocannabinoid levels, we studied their effects on anandamide cellular uptake and enzymatic hydrolysis. Although most of the compounds tested did inhibit anandamide metabolism (Table 4), particularly at the level of cellular uptake, their rank of potency (cannabichromene=cannabigerol>cannabidiol=THC) did not reflect their potency at inhibiting cancer cell proliferation.

To conclusively investigate the role of vanilloid TRPV1 receptors and cannabinoid CB_1 and CB_2 receptors in the anti-cancer effects of plant cannabinoids, in all those cell lines where cannabinoid or vanilloid receptors were expressed (Table 3), we studied the effect of selective antagonists, alone or in combination, on the inhibitory effect of 10 μM cannabidiol. Whereas 5'-iodo-resiniferatoxin (I-RTX, 100 nM) was used as a TRPV1 selective antagonist, and SR141716A (0.5 μM) and SR144528 (0.5 μM) were used as selective antagonists for CB_1 and CB_2 receptors, respectively. A statistically significant effect of selective concentrations of the two antagonists I-RTX and SR144528 was found only in MDA-MB-231 cells; however, these molecules were able to revert only partially the effect cannabidiol. Higher doses of the two compounds inhibited cell number *per se* and were not used. When I-RTX and SR144528 were administered together, cannabidiol effect was attenuated by about 40%, although this effect was probably minimized by the fact that the mixture of antagonists significantly inhibited cell growth *per se* (Fig. 6). These findings are in agreement with the results obtained by immunofluorescence and showing high levels of CB_2 and TRPV1 receptors in the plasma membrane of intact MDA-MB-231 cells (Fig. 7). Regarding the CB_1 antagonist, despite the presence in MDA-MB-231 cells of CB_1 receptors (Fig. 7), SR141716A (0.5 μM) did not influence the effect of cannabidiol (data not shown). No effect was observed with any of the three antagonists in the other cell lines, except for KiMol cells were the mixture of

antagonists showed a slight inhibition (15 ± 2%), which was not statistically significant (data not shown).

Role of vanilloid and cannabinoid receptors in MDA-MB-231 cells. Starting from the experiments with TRPV1, CB_1 and CB_2 receptor antagonists, we further investigated the role of direct or indirect activation of these receptors in cannabidiol effect on MDA-MB-231 cell growth. Cannabidiol and THC-A, tested at a 25 μM concentration, did inhibit the uptake of [^{14}C]anandamide by MDA-MB-231 cells (25.1 ± 2.5 and 21.0 ± 3.0% inhibition, respectively, mean ± SE; *n*=4), but cannabigerol and a selective inhibitor of anandamide cellular uptake, OMDM-2, were significantly more efficacious at exerting this effect (82.0 ± 3.5 and 77.0 ± 3.1% inhibition, respectively), even though they were significantly less efficacious than cannabidiol at inhibiting cell growth (Table 1 and data not shown). Furthermore, direct agonists of CB_1 and CB_2 receptors, i.e. arachidonoylchloroethanolamide and JWH-133, were also less potent and efficacious than cannabidiol at inhibiting MDA-MB-231 cell growth (data not shown). We also studied in MDA-MB-231 cells the effect of cannabidiol (5 μM) after a 10 min exposure to methyl-beta-cyclodextrin (0.5 mM), a potent membrane cholesterol depletor that is able to destroy the lipid rafts microdomains and to block the clustering of CB_1 at the plasma membrane in MDA-MB-231 cells (Sarnataro et al., 2005). We found no significant effect on the inhibitory action of cannabidiol (from 29.9 ± 3.5 to 30.2 ± 3.6% inhibition, mean ± SE; *n*=3; $p>0.05$).

Regarding TRPV1 receptors, we investigated whether cannabidiol induces intracellular Ca^{2+} elevation also in MDA-MB-231 cells. Cannabidiol did induce a rapid and sustained elevation of intracellular Ca^{2+} in MDA-MB-231 cells (EC_{50}=0.7 ± 0.1 μM, max. effect at 10 μM cannabidiol=14.5 ± 0.3% of the effect of 4 μM ionomycin, Fig. 8A,B) but in a way that was not blocked by I-RTX, nor by CB_1 or CB_2 receptor antagonists (Fig. 8D). In agreement with these data we also found that potent selective agonists of TRPV1 receptors, such as capsaicin and resiniferatoxin (RTX), respectively, exerted little effect on MDA-MB-231 cell growth (data not

shown). Moreover, cannabidiol effect on intracellular Ca^{2+} did not require the presence of extracellular Ca^{2+} (EC_{50}=1.3 ± 0.2 μM, Fig. 8C), indicating that it occurs mostly at the level of intracellular stores, and was in fact blocked after loading the cells with the Ca^{2+} chelating agent BAPTA-M (Fig. 8D).

Involvement of oxidative stress in CBD actions on MDA-MB-231 cells. MDA-MB-231 cells were selected also to investigate the implications of cannabidiol effects on oxidative stress phenomena. The effect of anti-oxidant agents on the anti-proliferative action of 10 μM cannabidiol were evaluated. Already at 0.1 μM concentration, α-tocopherol significantly prevented, although in a partial manner, the anti-proliferative effects of cannabidiol on these cells (Fig. 9A) and also vitamin C and astaxantine, at 25 μM concentration, were able to counteract the inhibitory effect of cannabidiol by ~30% (data not shown). Further experiments were performed to measure the intracellular ROS generation. Cannabidiol in a dose- and time-dependent manner induced ROS formation in MDA-MB-231 cells in a Ca^{2+}-containing buffer (Fig. 9B). Importantly, the effect of cannabidiol (10 μM) on ROS production (60 min) was Ca^{2+}–dependent as it was erased when cells were pre-loaded with BAPTA-M (40 μM) and incubated in an isotonic buffer with the same ionic strength but with Mg^{2+} instead of Ca^{2+} (Fig. 9B inset). Next, we carried out different incubations under both standard and severe growth cell culturing conditions that lead to a strong production of ROS, i.e. with 12 hours serum deprivation, and subsequently cells were treated either with low and high concentration of cannabidiol only for 24 hours, as opposed to the 96 hour incubation used in most of the experiments presented here. In non-serum deprived cells, cannabidiol exerted a pro-proliferative effect at low doses (0.5 μM), while it was ineffective after serum deprivation (Fig. 9A, B). At the highest concentration tested (10 μM) the growth inhibitory effect was much stronger than that caused by the same dose without serum deprivation (Fig. 10A, B). The effect of cannabidiol on ROS formation induced by 100 μM of H_2O_2 was also measured. In conformity with the results obtained in the short-term cell proliferation assays, cannabidiol, despite its stimulatory activity on

ROS formation when administered *per se* (Fig. 9B), was able to reduce ROS production induced by 100 μM of H_2O_2, but only at the lowest concentration tested (Fig.10C).

Discussion

The aim of this study was to identify natural cannabinoids with anti-tumor activities at least similar to those of THC, and devoid of the potential central effects of this compound. Given that the efficacy of cannabinoids as antitumoral agents appears to be strictly correlated to the cell type under investigation, we screened a panel of plant-cannabinoids in a wide range of tumoral cell lines distinct in origin and typology. We found that, surprisingly, cannabidiol acted as a more potent inhibitor of cancer cell growth than THC, and that cannabigerol and cannabichromene usually followed cannabidiol in the rank of potency. The cell growth inhibitory effect of cannabidiol depended on its chemical structure since the addition of a carboxylic acid group (as in cannabidiol-acid) dramatically reduced its activity. This is unlikely due to simple modification of the lipophilicity of the compound and subsequent decrease of its capability to penetrate the cell membrane, since THC-A was often more efficacious than THC. We also found that the cannabidiol-rich *Cannabis* extract was as potent as pure cannabidiol in most cases, or even more potent in some cell lines. These results suggest the use in cancer therapy for cannabidiol, a compound lacking the psychotropic effects typical of THC. Indeed, the efficacy of cannabidiol and of the cannabidiol-rich extract were confirmed in vivo in two different models of xenograft tumors obtained by inoculation in athymic mice of either v-K-*ras*-transformed thyroid epithelial cells or of the highly invasive MDA-MB-231 breast cancer cells. Furthermore, cannabidiol and the cannabidiol-rich extract also inhibited the formation of lung metastases subsequent to inoculation of MDA-MB-231 cells, in agreement with the inhibitory actions on cancer cell migration previously described for this compound (Vaccani et al., 2005).

The weak effects observed here with THC might be regarded as surprising. In fact, THC was reported to induce apoptosis in both C_6 glioma and human prostate PC-3 cells (Sanchez et al., 1998; Ruiz et al., 1999), although it may even enhance breast cancer growth and metastasis (McKallip et al., 2005). The low potency found here for this compound, at least in glioma and prostate cancer, could be explained by the different experimental conditions used, and supports the notion that the

efficacy of cannabinoids is strongly dependent on the cell type utilized. In fact, regarding glioma cells, THC-induction of apoptosis was reported not in C_6 cells, but in a THC-sensitive subclone ($C_{6.9}$). Furthermore, Ruiz et al. (1999) used a human prostate cancer cell line different from the one used here. Melck et al. (2000) found that stimulation of CB_1 receptors causes inhibition of DU-145 cell proliferation only when this is induced by nerve growth factor. Using similar culturing conditions as those used here, we previously showed that CB_1, but not CB_2, stimulation inhibits the proliferation of MCF-7, KiMol and CaCo-2 cells more potently than what observed here with THC (De Petrocellis et al., 1998; Bifulco et al., 2001; Ligresti et al., 2003). This might be due to the use in those studies of CB_1 agonists with higher potency or efficacy than THC, or of cells clones with a higher expression of CB_1 receptors than that observed here. Indeed, McKallip et al. (2005) proposed for human breast cancer cells that resistance to THC toxicity is correlated to low expression of CB_1 receptors and high expression of vanilloid receptors.

To date, the receptor-mediated anti-cancer effects of cannabinoids and endocannabinoids have been ascribed to either CB_1-mediated inhibition of mitosis, as in the case of some hormone-sensitive cells, or to the induction of apoptosis following activation of TRPV1 and/or CB_2 receptors. Starting from the hypothesis that cannabidiol decreased cell number by induction of apoptosis at least for human glioma cell lines (Massi et al., 2004), we decided to evaluate the percent of apoptotic cells after exposure to cannabidiol and found that the effect of the compound was due to an arrest of the cell cycle in the case of MCF-7 (hormone-sensitive) cells, to both cell cycle arrest and apoptosis in KiMol cells (which are also hormone-sensitive to some extent), and only to induction of apoptosis in C_6 and MDA-MB-231 (non-hormone-sensitive) cells. It was, therefore, clear that cannabidiol lacks a unique mode of action for its anti-cancer effect on the cell lines under investigation. Based on previous evidence that cannabidiol, although inactive as a direct agonist at cannabinoid CB_1 and CB_2 receptors, activates directly the vanilloid TRPV1 receptor and is capable of increasing endocannabinoid levels by inhibiting their inactivation (Bisogno et al., 2001), we first investigated the capability of plant cannabinoids to interact with the key components

of the endocannabinoid or endovanilloid systems. Indeed, cannabidiol, cannabigerol and cannabichromene were found here to activate TRPV1 receptors and/or inhibit anandamide inactivation to some extent. However, despite the presence of either cannabinoid or vanilloid receptors (or both) in all cell lines under study, in none but one of these cell lines the direct or indirect stimulation of these receptors seemed to be entirely or even partially responsible for the anti-cancer effects of cannabidiol. The only important exception was represented by MDA-MB-231 cells, where a partial, although significant, reversion of the effect of cannabidiol was observed in the presence of selective antagonists for TRPV1 and CB_2 receptors, thus pointing to the partial involvement of these receptors in the anti-cancer action of this cannabinoid in breast carcinoma cells. This finding is important in view of the fact that these cells were the ones used in the present study to investigate the anti-cancer and anti-metastatic effects of cannabidiol in vivo. However, the present observation that "pure" agonists of CB_2 and TRPV1 receptors, or a selective inhibitor of anandamide uptake, were less efficacious than cannabidiol at inhibiting MDA-MB-231 cell growth strongly suggests that the two receptors act cooperatively with other mechanisms at inducing apoptosis, and that other unique effects of cannabidiol also contribute to its anti-cancer actions.

It has been reported that plant and endogenous cannabinoids can induce apoptosis through several molecular mechanisms (Galve-Ropher et al., 2000; Jacobsson et al., 2001). When TRPV1 is involved, apoptosis is induced by mithocondrial events triggered by TRPV1-mediated calcium influx (Maccarrone et al., 2000), whereas when CB_2 receptors are involved, ceramide accumulation seems to be the most important intracellular event causing programmed cell death (Galve-Ropher et al., 2000). Our data indicate that a part of the pro-apoptotic effect of cannabidiol in MDA-MB-231 cells might be due to these mechanisms. However, a TRPV1- and CB_2-independent mechanism known to induce apoptosis is the rise of intracellular ROS levels, as demonstrated by the fact that non-vanilloid-, non-cannabinoid receptor-mediated anandamide-induced apoptosis is prevented by antioxidant agents (Sarker et al., 2000). Hence, the effect of cannabidiol might also be attributed to ROS production. For this reason we investigated the involvement of oxidative stress in cannabidiol

effects in MDA-MB-231 cells. We found that antioxidants attenuated the pro-apoptotic effects of cannabidiol in these cells, suggesting that this compound is indeed capable of exerting pro-oxidative properties at least in tumor cell lines. Importantly, the extent of the effect of the anti-oxidants accounted for that part of cannabidiol action that was not blocked by CB_2 and TRPV1 receptor antagonists. Accordingly, cannabidiol, at the concentrations exerting anti-proliferative effects, also induces a significant enhancement of ROS levels in MDA-MB-231 cells. The capability of cannabidiol to induce ROS might be surprising in view of its phenolic chemical structure, which would rather favor an inhibitory effect on oxidative stress. However, we provided here data suggesting that cannabidiol might cause ROS elevation indirectly, i.e. by elevating intracellular Ca^{2+}. Cannabidiol-induced intracellular Ca^{2+} elevation occurred in the same range of concentrations as those necessary to cause growth inhibition, was independent of TRPV1, CB_1 and CB_2 receptor activation, and might be related to the analogous effect recently observed with THC, cannabinol and cannabidiol in T cells (Rao and Kaminski, 2006). Finally, at a submicromolar concentration, cannabidiol was also capable of inhibiting H_2O_2-induced ROS formation, similar to what observed previously in non-tumor cells (Hampson et al., 1998; Iuvone et al., 2004), thus possibly explaining why also in the present study, in certain cells and at low concentrations, or with short incubation times and in cell culturing conditions in which not so many ROS are present (i.e. in the presence of serum), this compound can also produce pro-proliferative effects.

In conclusion, our data indicate that cannabidiol, and possibly *Cannabis* extracts enriched in this natural cannabinoid, represent a promising non-psychoactive antineoplastic strategy. In particular, for a highly malignant human breast carcinoma cell line we have shown here that cannabidiol and a cannabidiol-rich extract counteract cell growth both in vivo and in vitro as well as tumor metastasis in vivo. Cannabidiol exerts its effects on these cells through a combination of mechanisms that include either direct or indirect activation of CB_2 and TRPV1 receptors, and induction of oxidative stress, all contributing to induce apoptosis. Additional investigations are

required to understand the mechanism of the growth inhibitory action of cannabidiol in the other cancer cell lines studied here.

Acknowledgments. The authors are grateful to Prof. Teresa Iuvone and Dr. Daniele De Filippis for their valuable help with caspase-3 data, and to Dr. Tiziana Bisogno for her critical comments and general contribution to this work.

References

Bifulco M, Laezza C, Portella G, Vitale M, Orlando P, De Petrocellis L and Di Marzo V (2001) Control by the endogenous cannabinoid system of ras oncogene-dependent tumor growth. *FASEB J*. **15:**2745-2747.

Bifulco M and Di Marzo V (2002) Targeting the endocannabinoid system in cancer therapy: a call for further research. *Nat. Med.* **8:**547-550. Review.

Bifulco M, Laezza C, Valenti M, Ligresti A, Portella G and Di Marzo V (2004) A new strategy to block tumor growth by inhibiting endocannabinoid inactivation. *FASEB J.* **18:**1606-1608.

Bisogno T, Hanus L, De Petrocellis L, Tchilibon S, Ponde DE, Brandi I, Moriello AS, Davis JB, Mechoulam R and Di Marzo V (2001) Molecular targets for cannabidiol and its synthetic analogues: effect on vanilloid VR1 receptors and on the cellular uptake and enzymatic hydrolysis of anandamide. *Br. J. Pharmacol*. **134:**845-852.

Bornheim LM, Grillo MP. (1998) Characterization of cytochrome P450 3A inactivation by cannabidiol: possible involvement of cannabidiol-hydroxyquinone as a P450 inactivator. *Chem Res Toxicol*. **11:**1209-1216.

Casanova ML, Blazquez C, Martinez-Palacio J, Villanueva C, Fernandez-Acenero MJ, Huffman JW, Jorcano JL and Guzman M (2003) Inhibition of skin tumor growth and angiogenesis in vivo by activation of cannabinoid receptors. *J. Clin. Invest.* **111:** 43-50.

Colasanti BK. (1990) A comparison of the ocular and central effects of delta 9-tetrahydrocannabinol and cannabigerol. *J Ocul Pharmacol*. **6:**259-269.

Contassot E, Tenan M, Schnuriger V, Pelte MF and Dietrich PY (2004) Arachidonyl ethanolamide induces apoptosis of uterine cervix cancer cells via aberrantly expressed vanilloid receptor-1. *Gynecol. Oncol*. **93:**182-188.

De Petrocellis L, Bisogno T, Davis JB, Pertwee RG and Di Marzo V (2000) Overlap between the ligand recognition properties of the anandamide transporter and the VR1 vanilloid receptor: inhibitors of anandamide uptake with negligible capsaicin-like activity. *FEBS Lett.* **483:**52-56.

De Petrocellis L, Melck D, Palmisano A, Bisogno T, Laezza C, Bifulco M and Di Marzo V (1998) The endogenous cannabinoid anandamide inhibits human breast cancer cell proliferation. *Proc. Natl. Acad. Sci. U S A.* **95:** 8375-8380.

Galve-Roperh I, Sanchez C, Cortes ML, del Pulgar TG, Izquierdo M and Guzman M (2000) Anti-tumoral action of cannabinoids: involvement of sustained ceramide accumulation and extracellular signal-regulated kinase activation. *Nat. Med.* **6:**313-319.

Gaoni Y and Mechoulam R (1964) Isolation, structure and partial synthesis of an active constituent of hashish. *J. Am. Chem. Soc.* **86:**1646-1647.

Guzman M (2003) Cannabinoids: potential anticancer agents. *Nat. Rev. Cancer*. **3:**745-755. Review.

Hampson AJ, Grimaldi M, Axelrod J and Wink D (1998) Cannabidiol and (-)Delta9-tetrahydrocannabinol are neuroprotective antioxidants. *Proc. Natl. Acad. Sci. U S A.* **95:** 8268-8273.

Ilan AB, Gevins A, Coleman M, ElSohly MA, de Wit H. (2005) Neurophysiological and subjective profile of marijuana with varying concentrations of cannabinoids. *Behav Pharmacol*. **16:**487-496.

Iuvone T, Esposito G, Esposito R, Santamaria R, Di Rosa M and Izzo AA (2004) Neuroprotective effect of cannabidiol, a non-psychoactive component from *Cannabis* sativa, on beta-amyloid-induced toxicity in PC12 cells. *J. Neurochem.* **89:**134-141.

Jacobsson SO, Wallin T and Fowler CJ (2001) Inhibition of rat C_6 glioma cell proliferation by endogenous and synthetic cannabinoids. Relative involvement of cannabinoid and vanilloid receptors. *J. Pharmacol. Exp. Ther*. **299:** 951-959.

Kogan NM (2005) Cannabinoids and cancer. *Mini. Rev. Med. Chem*. **5**:941-952.

Ligresti A, Bisogno T, Matias I, De Petrocellis L, Cascio MG, Cosenza V, D'Argenio G, Scaglione G, Bifulco M, Sorrentini I and Di Marzo V (2003) Possible endocannabinoid control of colorectal cancer growth. *Gastroenterology*. **125:**677-687.

Maccarrone M, Lorenzon T, Bari M, Melino G and Finazzi-Agro A (2000) Anandamide induces apoptosis in human cells via vanilloid receptors. Evidence for a protective role of cannabinoid receptors. *J. Biol. Chem.* **275:**31938-31945.

Massi P, Vaccani A, Ceruti S, Colombo A, Abbracchio MP and Parolaro D (2004) Antitumor effects of cannabidiol, a nonpsychoactive cannabinoid, on human glioma cell lines. *J. Pharmacol. Exp. Ther*. **308:**838-845.

McKallip RJ, Nagarkatti M and Nagarkatti PS (2005) Delta-9-tetrahydrocannabinol enhances breast cancer growth and metastasis by suppression of the antitumor immune response. *J. Immunol.* **174:**3281-3289.

Melck D, De Petrocellis L, Orlando P, Bisogno T, Laezza C, Bifulco M and Di Marzo V (2000) Suppression of nerve growth factor Trk receptors and prolactin receptors by endocannabinoids leads to inhibition of human breast and prostate cancer cell proliferation. *Endocrinology*. **141:**118-126.

Mechoulam R, Parker LA and Gallily R (2002) Cannabidiol: an overview of some pharmacological aspects. *J. Clin. Pharmacol*., **42**(11 Suppl):11S-19S.

Mimeault M, Pommery N, Wattez N, Bailly C and Henichart JP (2003) Anti-proliferative and apoptotic effects of anandamide in human prostatic cancer cell lines: implication of epidermal growth factor receptor down-regulation and ceramide production. *Prostate*. **56:**1-12.

Ortar G, Ligresti A, De Petrocellis L, Morera E, Di Marzo V. (2003) Novel selective and metabolically stable inhibitors of anandamide cellular uptake. *Biochem Pharmacol*. **65:**1473-1481.

Pertwee RG (1997) Pharmacology of cannabinoid CB1 and CB2 receptors. *Pharmacol. Ther.* **74:**129-180. Review.

Pertwee RG (2004) The pharmacology and therapeutic potential of cannabidiol. In “Cannabinoids” V. Di Marzo Ed., Kluwer Academic/Plenum Publishers, New York, pp. 32-83.

Rao GK and Kaminski NE (2006) Cannabinoid-mediated elevation of intracellular calcium: a structure-activity relationship. *J. Pharmacol. Exp. Ther*. **317**:820-829.

Robson P. (2005) Human studies of cannabinoids and medicinal cannabis. *Handb Exp Pharmacol.* **168:**719-756. Review.

Ruiz L, Miguel A and Diaz-Laviada I (1999) Delta9-tetrahydrocannabinol induces apoptosis in human prostate PC-3 cells via a receptor-independent mechanism. *FEBS Lett.* **458:**400-404.

Russo E and Guy GW (2006) A tale of two cannabinoids: The therapeutic rationale for combining tetrahydrocannabinol and cannabidiol. *Med. Hypotheses.* **66:**234-246.

Sanchez C, Galve-Ropher I, Canova C, Brachet P and Guzman M (1998) Delta9-tetrahydrocannabinol induces apoptosis in C_6 glioma cells. *FEBS Lett.* **436:** 6-10.

Sanchez C, de Ceballos ML, del Pulgar TG, Rueda D, Corbacho C, Velasco G, Galve-Roperh I, Huffman JW, Ramon y Cajal S and Guzman M (2001) Inhibition of glioma growth in vivo by selective activation of the CB(2) cannabinoid receptor. *Cancer Res.* **61:**5784-5789.

Sanchez MG, Sanchez AM, Ruiz-Llorente L and Diaz-Laviada I (2003) Enhancement of androgen receptor expression induced by (R)-methanandamide in prostate LNCaP cells. *FEBS Lett.* **555:**561-566.

Sarfaraz S, Afaq F, Adhami VM and Mukhtar H (2005) Cannabinoid receptor as a novel target for the treatment of prostate cancer. *Cancer Res.* **65:**1635-1641.

Sarker KP, Obara S, Nakata M, Kitajima I and Maruyama I (2000) Anandamide induces apoptosis of PC-12 cells: involvement of superoxide and caspase-3. *FEBS Lett.* **472:** 39-44.

Sarnataro D, Grimaldi C, Pisanti S, Gazzerro P, Laezza C, Zurzolo C and Bifulco M (2005) Plasma membrane and lysosomal localization of CB1 cannabinoid receptor are dependent on lipid rafts and regulated by anandamide in human breast cancer cells. *FEBS Lett.* **579:**6343-6349.

Vaccani A, Massi P, Colombo A, Rubino T and Parolaro D (2005) Cannabidiol inhibits human glioma cell migration through a cannabinoid receptor-independent mechanism. *Br. J. Pharmacol.* **144:**1032-1036.

Walsh D, Nelson KA and Mahmoud FA (2003) Established and potential therapeutic applications of cannabinoids in oncology. *Support Care Cancer.* **11:**137-143.

Footnotes

This study was supported by a research grant from GW Pharmaceuticals (to VDM).

Legends for Figures

Figure 1: Chemical structures of the plant-derived cannabinoids used in this study.

Figure 2: Effect of cannabinoids and *Cannabis* extracts on the proliferation of some of the cell lines investigated in this study. MCF-7 cells (**A**), C_6 cells (**B**) and DU-145 cells (**C** and **D**) were treated with increasing concentrations of cannabidiol, cannabinoids (**C**) and cannabidiol-rich extracts (daily added with each change of medium for 4 days). Effect on cell proliferation was measured by Crystal Violet vital staining. After staining, cells were lysated in 0.01% of Acetic Acid and analyzed by spectrophotometric analysis (Perkin Elmer Lambda 12, λ=595nm). Results are reported as percent of inhibition of proliferation where OD value from vehicle-treated cells was considered as 100% of proliferation and represent the mean ± SE of three different experiments. ($*$, $p< 0.05$ vs, cannabidiol pure by ANOVA followed by Bonferroni's test). (**E**, **F**) Effect of cannabidiol on non-tumoral cell lines. Cells were treated with two different concentrations of cannabidiol for four days (**E**) or three days (**F**) and vitality was evaluated by using Trypan Blue dye-exclusion assay (see *Materials and Methods*). In cells treated with vehicle, mortality was always lower than 2%. Data are expressed as % of control and represent the mean ± SE of three different experiments. Statistical analysis was carried out by ANOVA followed by Bonferroni's test (** $p< 0.01$, *** $p<0.001$ *vs*. the same concentration of cannabidiol on MDA-MB-231 cells). CBD, cannabidiol; CBG, cannabigerol; CBC, cannabichromene; CBD-A, cannabidiol-acid; THC-A, THC-acid; CBD-rich, cannabidiol-enriched cannabis extract; THC-rich, THC-enriched cannabis extract.

Figure 3: In vivo actions of cannabidiol on tumor growth and metastasis. (**A**, **B**) Effect of cannabidiol (5mg/kg) and cannabidiol-rich extract (6.5mg/kg) on two different xenograft tumor models in athymic mice. KiMol cells (**A**) or MBA-MD-231 cells (**B**) were injected s.c. (day 0 of treatment) into the dorsal right side of athymic mice and the intra-tumor treatments administered twice per week. Results represent mean ± SE ($*$, $p< 0.05$ vs. Vehicle; $n= 6$ by ANOVA followed by Bonferroni's test). (**C**) Effect of cannabidiol and cannabidiol-rich extract on breast cancer cell metastasis. MDA-MB-231 cells were injected into the left paw of 30-day-old BalB/c male mice.

Animals were divided into three groups (*n*=11 for vehicle; *n*= 14 for treated) and treated with vehicle (CTR), cannabidiol (5 mg/kg/dose) or cannabidiol-rich extract (6.5 mg/kg/dose). The drugs were injected i.p. every 72 hours. Lung metastatic nodules were evaluated 21 days after the injection. Data represent mean ± SE of number of nodules (*, $p< 0.05$; **, $p< 0.01$ *vs* CTR). Statistical analysis was performed by ANOVA followed by Bonferroni's test. CBD, cannabidiol; CBD-rich, cannabidiol-enriched cannabis extract.

Figure 4: (A-D) Representative FACS analyses showing the effect of 2 days treatment of 10 μM cannabidiol (CBD) on apoptosis rate in various cell lines calculated as the percentage of cells showing a subdiploid DNA peak (sub-G1). Graphs are representative of three independent experiments with similar results. Graphs on the left are from cells treated with vehicle and those on the right from cells treated with cannabidiol. Line bar shows where the subdiploid DNA peak is calculated. CTR= vehicle-treated cells. (**E**) Effect of cannabidiol on caspase 3 release from pro-caspase. Western immunoblotting analysis was performed to detect the levels of caspase-3 expression. Proteins were extracted from DU-145 cells (lanes 1 and 2) or MDA-MB-231 cells (lanes 3 and 4) treated with vehicle (CTR, lanes 1 and 3) or 10μM cannabidiol (cannabidiol, lanes 2 and 4) for 48 hours. Determination of relative band intensity was carried out using a GS700 densitometer and the results are presented in arbitrary scanning units. DU-145**:** CTR= 5.7 ± 0.81; cannabidiol= 4.2 ± 0.74 MDA-MB-231**:** CTR= 3.11 ± 0.67; cannabidiol= 2.64 ± 0.26 (Procaspase), 2.89 ± 0.51 (Caspase), mean ± SE of *n*=3 separate experiments.

Figure 5: Effect of plant cannabinoids and *Cannabis* extracts on vanilloid TRPV1 receptor activation. Human embryonic kidney (HEK 293) cells over-expressing the human recombinant TRPV1 receptor were loaded with a selective fluorescent probe (see *Materials and Methods*). The TRPV1-mediated effect on $[Ca^{2+}]_i$ was determined by measuring cell fluorescence before and after the addition of the test compounds at increasing concentrations. Data are reported as percent of the maximal effect obtained with Ionomycin 4μM, and are means of n=3 separate experiments. Error

bars are not shown for the sake of clarity and were never higher than 5% of the means. CBD, cannabidiol; CBG, cannabigerol; CBC, cannabichromene; CBD-A, cananbidiol-acid; THC-A, THC-acid; CBD-rich, cannabidiol-enriched cannabis extract; THC-rich, THC-enriched cannabis extract.

Figure 6: Influence of selective receptor antagonists on cannabidiol (CBD) anti-proliferative action. MDA-MB-231 cells were treated with 10μM cannabidiol in presence or in absence of selective antagonist for CB_2 receptors (0.5μM SR144528, denoted as SR_2), TRPV1 receptors (100nM 5'-I-resiniferatoxin denoted as I-RTX) or a mixture of both compounds (mix). Data are shown as percent inhibition of proliferation. Cells vehicle-treated were used as 100% of proliferation. (*, $p<0.05$ vs. cannabidiol only, by ANOVA followed by Bonferroni's test).

Figure 7: Representative photomicrographs demonstrating localization of CB_1, CB_2 and TRPV1 receptors in human breast adenocarcinoma (MDA-MB-231) cells as determined by the immunofluorescence technique described under *Materials and Methods*. (**A**) CB_1 receptor immunoreactivity. (**B**) CB_2 receptor immunoreactivity. (**C**) TRPV1-immunoreactivity. was performed using rabbit polyclonal anti-CB_1, anti-CB_2 (both diluted 1:50) and AlexaFluor488-conjugated secondary antibody (1:100) and goat polyclonal anti-TRPV1 diluted 1:100 and AlexaFluor546 conjugated secondary antibody (1:200). Magnification: 63x. Scale bar: 40 μm. Immunofluorescence was almost undetectable when pre-incubating antibodies with the corresponding blocking peptides (not shown).

Figure 8: Effect of cannabidiol (CBD) on intracellular Ca^{2+} in MDA-MB-231 cells. (**A**) Dose-related effect of cannabidiol in the presence of extracellular Ca^{2+}, as determined with Fluo-4. Data are mean ± SE of n=4 experiments and are expressed as % of the effect obtained with 4 μM ionomycin. (**B**) Time-related effect of cannabidiol (10 μM) in the presence of extracellular Ca^{2+}. Trace is representative of n=4 experiments. (**C**) Dose-related effect of cannabidiol in the absence of extracellular Ca^{2+}, as determined with Fura-2. Data are mean ± SE of n=4 experiments. Maximal $\Delta_{fluorescence}$ was 0.235±0.031 at 10 μM cannabidiol and was usually attained after 200 sec (**D**). Effect

of various antagonists (the CB_1 antagonist AM251, 1 μM; the CB_2 antagonist AM630, 1 μM; the TRPV1 antagonist 5'-I-resiniferatoxin [I-RTX], 0.1 μM; 5 min pre-treatment) and the intracellular calcium chelating agent BAPTA-M (20 μM, loaded onto the cells before stimulation) on cannabidiol (1 μM) action on intracellular Ca^{2+}. Similar results were obtained with SR141716A and SR144528.

Figure 9: Study of the involvement of oxidative stress in the effect of cannabidiol (CBD). (**A**) The anti proliferative effect of 10μM cannabidiol on MDA-MB-231 cells was measured after four days of treatment in absence or in presence of increasing concentrations of α-tocopherol. Data represent mean ± SE of % inhibition of proliferation (*, $p< 0.05$ by ANOVA followed by Bonferroni's test). (**B**) Time course of ROS production by MDA-MB-231 cells ($16x10^3$ cells/well) as measured by spectrofluorimetric analysis. Cells were loaded 1 hour with 10μM of fluorescent probe in presence of 0.05% Pluronic; fluorescence was measured in a 96 wells microplate reader (Perkin Elmer LS50B, λ_{Ex} 495nm - λ_{Em} 521nm). Fluorescence detection was carried out after the incubation of either 100 μM H_2O_2 or increasing concentrations of cannabidiol at different times (0-30-60-120 minutes). 100 μM H_2O_2 was used as a positive control in these experiments. The fluorescence measured at time zero was considered as basal ROS production and subtracted from the fluorescence at different times (Δ_1). Data are reported as Δ_2, i.e. Δ_1 values at different doses subtracted of the Δ_1 values of cells incubated with vehicle, and are mean ± SE of n=3 experiments. The effects of H_2O_2 and of all doses of cannabidiol were significantly different from control values as determined by ANOVA followed by Bonferroni's test. In the inset, the lack of effect of cannabidiol 10 μM on ROS production (after 60 min) in the absence of both extracellular and intracellular Ca^{2+} is shown. ***, $p<0.005$ by ANOVA, n=5.

Figure 10: Study of the involvement of oxidative stress in the effect of cannabidiol (CBD). (**A-B**) The anti-proliferative effect of cannabidiol was evaluated in standard growth conditions or after 12 hours of serum deprivation to induce oxidative stress. Post-starvation, cells were treated with 0.5 or

10 μM cannabidiol for 24 hours and the effect on proliferation was evaluated by Crystal Violet staining. Data are reported as mean ± SE of % inhibition of proliferation, *n*=3. (**C**) ROS production after 2 hours of incubations with cannabidiol or H_2O_2 was measured in MDA-MB-231 cells ($16x10^3$cells/well) by spectrofluorimetric analysis. The effect of cannabidiol *per se* (0.5 and 10 μM) is reported in Fig. 9. Cells were loaded 1 hour with 10 μM of fluorescent probe in presence of 0.05% Pluronic and fluorescence was measured in a 96 wells microplate reader (Perkin Elmer LS50B, λ_{Ex} 495nm - λ_{Em} 521nm). Fluorescence was measured at T=0 and after 2 hours of incubation with H_2O_2 in presence or in absence of increasing concentration of cannabidiol. Data are expressed as explained in the legend to Figure 9. Cannabidiol inhibited ROS production by H_2O_2 only at the lowest concentration (0.5 μM, $p<0.05$ by ANOVA followed by Bonferroni's test).

Table 1: Effect of cannabinoids and *Cannabis* extracts on cancer cell growth. Various epithelial cell lines of various tumoral origin were treated with different concentrations of drugs and after four days the cell number was measured with Crystal Violet Vital staining (see *Materials and Methods*). Data are reported as mean ± SE of IC_{50} values (μM) calculated from three independent experiments. CBD, cannabidiol; CBG, cannabigerol; CBC, cannabichromene; CBD-A, cannabidiol-acid; THC-A, THC-acid; CBD-rich, cannabidiol-enriched cannabis extract; THC-rich, THC-enriched cannabis extract.

	MCF-7	**C_6**	**DU-145**	**KiMol**	**CaCo-2**	**MDA-MB-231**	**RBL-2H3**	**AGS**
Δ^9-THC	14.2 ± 2.1	23.0 ± 4.2	>25	23.2 ± 1.5	16.5 ± 0.2	24.3 ± 4.2	15.8 ± 3.7	19.3 ± 1.5
THC-A	9.8 ± 0.4	18.0 ± 5.3	>25	21.0 ± 2.7	21.5 ± 1.4	18.2 ± 5.3	10.0 ± 3.4	> 25
CBD	8.2 ± 0.3	8.5 ± 0.8	20.2 ± 1.8	6.0 ± 3.0	7.5 ± 0.5	10.6 ± 1.8	6.3 ± 1.5	7.5 ± 1.3
CBD-A	21.7 ± 3.2	18.0 ± 4.2	>25	12.7 ± 3.0	>25	>25	>25	>25
CBG	9.8 ± 3.4	13.0± 2.1	21.3± 1.7	8.2 ± 0.7	9.0 ± 1.4	16.2 ± 2.1	9.0 ± 0.7	8.2 ± 0.7
CBC	14.2 ± 1.4	13.0 ± 2.6	>25	7.3 ± 3.0	12.0 ± 2.4	20.4 ± 2.6	15.8 ± 4.2	18.3 ± 3.0
THC-rich	21.0 ± 0.5	18.5 ± 3.3	>25	23.0 ± 2.0	16.0 ± 0.5	25.2 ± 3.3	14.6 ± 3.1	22.0 ± 2.0
CBD-rich	6.0 ± 1.0	4.7 ± 0.6	20 ± 4.6	6.2 ± 2.9	12.3 ± 1.2	14.1 ± 1.6	7.0 ± 0.6	10.0 ± 1.9

Table 2: Determination of of cell cycle arrest, apoptosis and mortality in the various cell lines exposed for 48 hours to 10 μM of cannabidiol before flow cytometry analysis (see Figure 4 and *Materials and Methods)*. Each experiment was repeated three times.

CELL TYPE	CELL CYCLE ARREST	APOPTOSIS	MORTALITY
DU-145	**ABSENT**	**<10**	**ABSENT**
MCF-7	**G1/S**	**ABSENT**	**ABSENT**
C_6	**ABSENT**	**9-10%**	**25-27%**
KIMOL	**G1/S**	**12-15%**	**20-22%**
MDA-MB-231	**ABSENT**	**15%**	**ABSENT**

Table 3: Schematic and qualitative representation of the results of the RT-PCR analyses of mRNAs for cannabinoid and vanilloid receptors in the cell lines under study. Total RNA from cells was extracted and its integrity was verified. RNA was further treated with RNAse-free DNAse I (Ambion DNA-freeTM kit) to digest contaminating genomic DNA and to subsequently remove the DNAse and divalent cations. The expression of mRNAs was examined by RT-PCR. Transcripts for FAAH, CB_1 and CB_2 receptors were analyzed and are classified as: a=abundant; m=medium; w=weak; nd=not detected, based on the intensity of the band normalized to the band corresponding to glyceraldehyde-3-phosphate dehydrogenase as the housekeeping gene, and on the number of cycles necessary to obtain a visible band. Results are based on *n*=3 separate determinations.

Cell type	CB_1	CB_2	TRPV1
AGS	nd	nd	a
DU-145	a	w	a
MCF-7	w	w	a
C_6	m	w	m
KiMol	w	a	m
CaCo-2	w	a	a
RBL-2H3	nd	a	nd
MDA-MB-231	w	m	a

Table 4: Effect of plant cannabinoids on anandamide inactivation. Membranes from N18TG2 cells were incubated with [^{14}C]anandamide in presence of compounds for 30 min at 37°C (see *Material and Methods*) to determine the effect on the enzymatic hydrolysis by fatty acid amide hydrolase (FAAH). Intact RBL-2H3 cells were incubated with [^{14}C]anandamide in presence of compounds for 5 min at 37°C (see *Material and Methods*) to determine the effect on anandamide cellular uptake (ACU). Data represent mean ± SE of three different experiments. [a]data from Bisogno et al., 2001. CBD, cannabidiol; CBG, cannabigerol; CBC, cannabichromene; CBD-A, cannabidiol-acid; THC-A, THC-acid.

	FAAH assay IC_{50} (μM)	**ACU assay IC_{50} (μM)**
THC	>50	22 ± 5
CBD	28 ± 3[a]	22 ± 2 [a]
CBG	>50	15 ± 3
CBC	>50	13 ± 2
THC-A	>50	>25
CBD-A	>50	>25

Figure 1

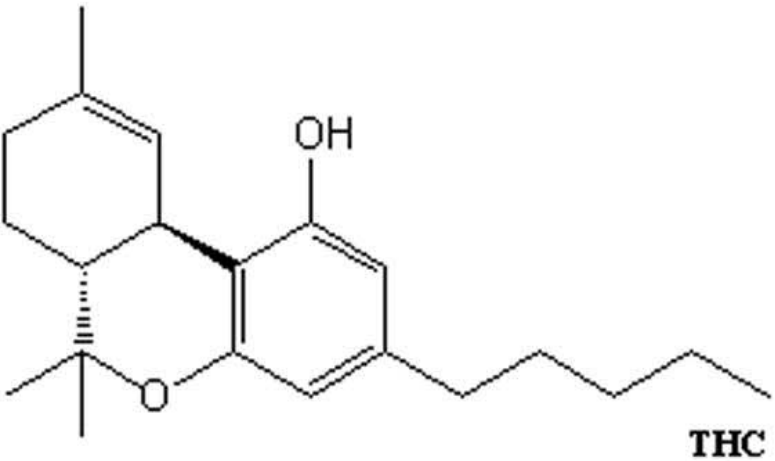

THC

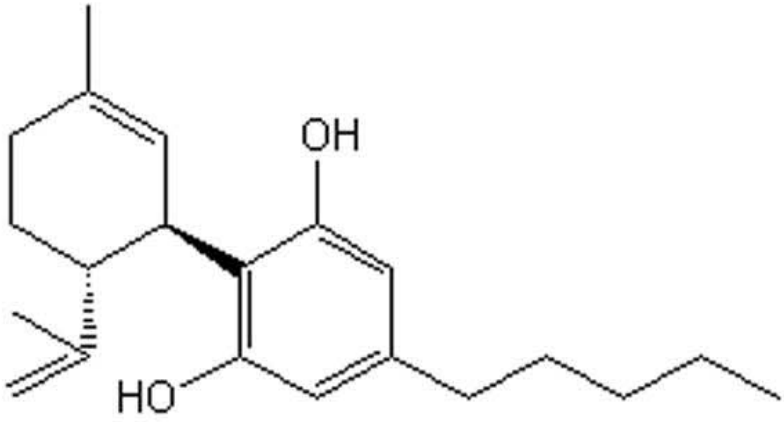

CBD

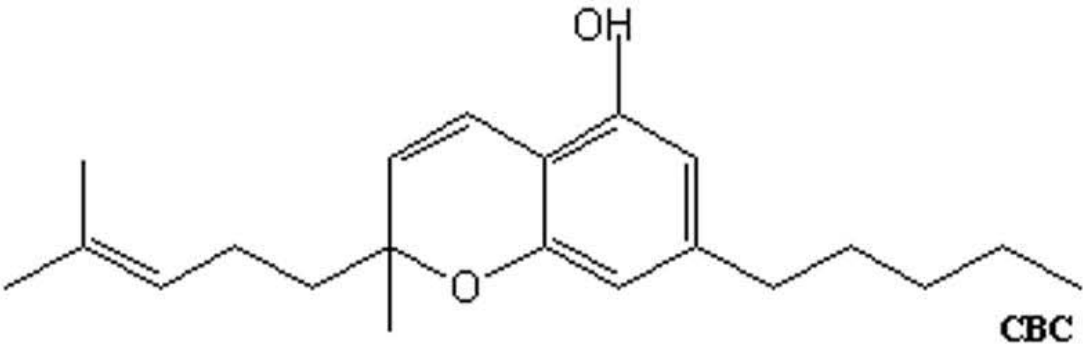

CBC

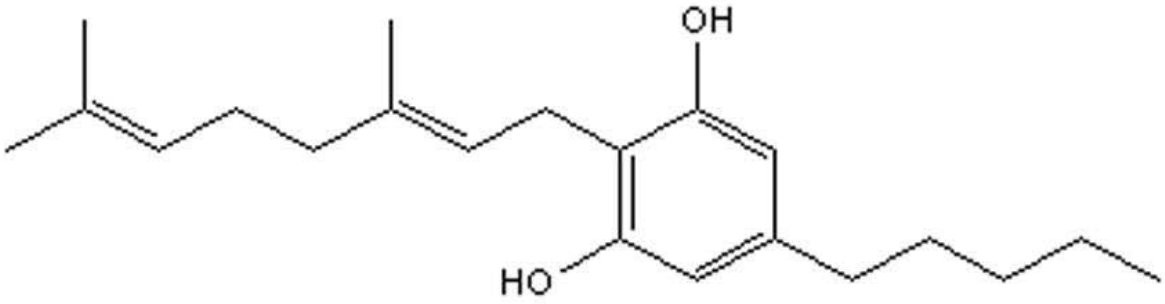

CBG

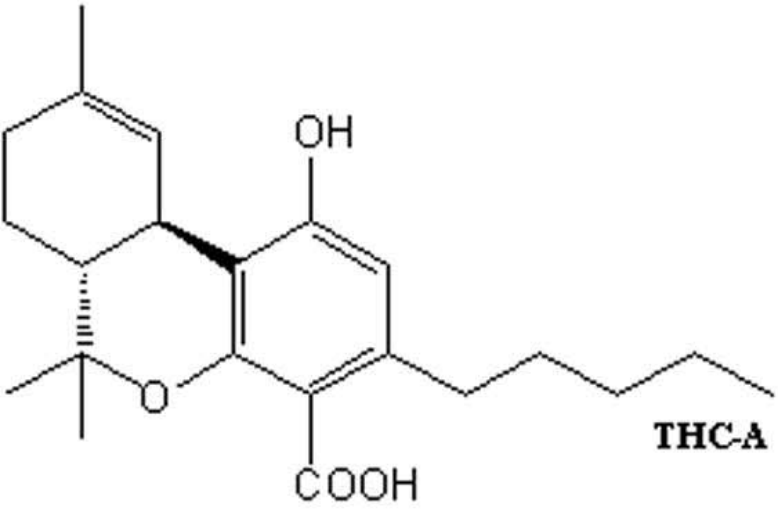

THC-A

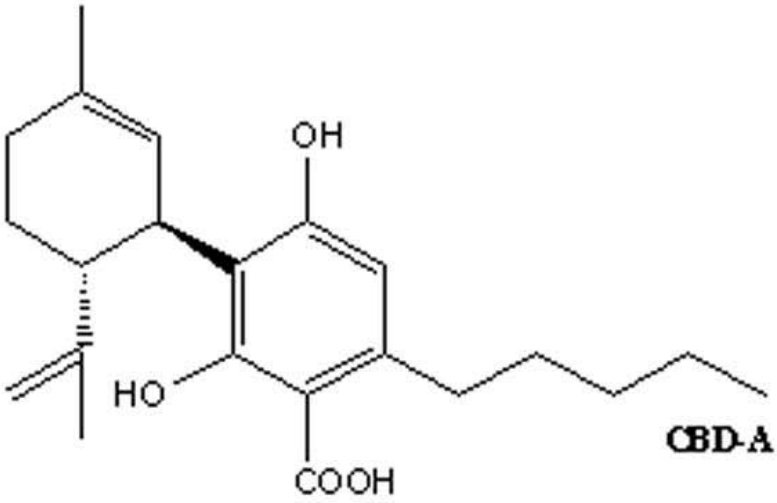

CBD-A

Figure 2

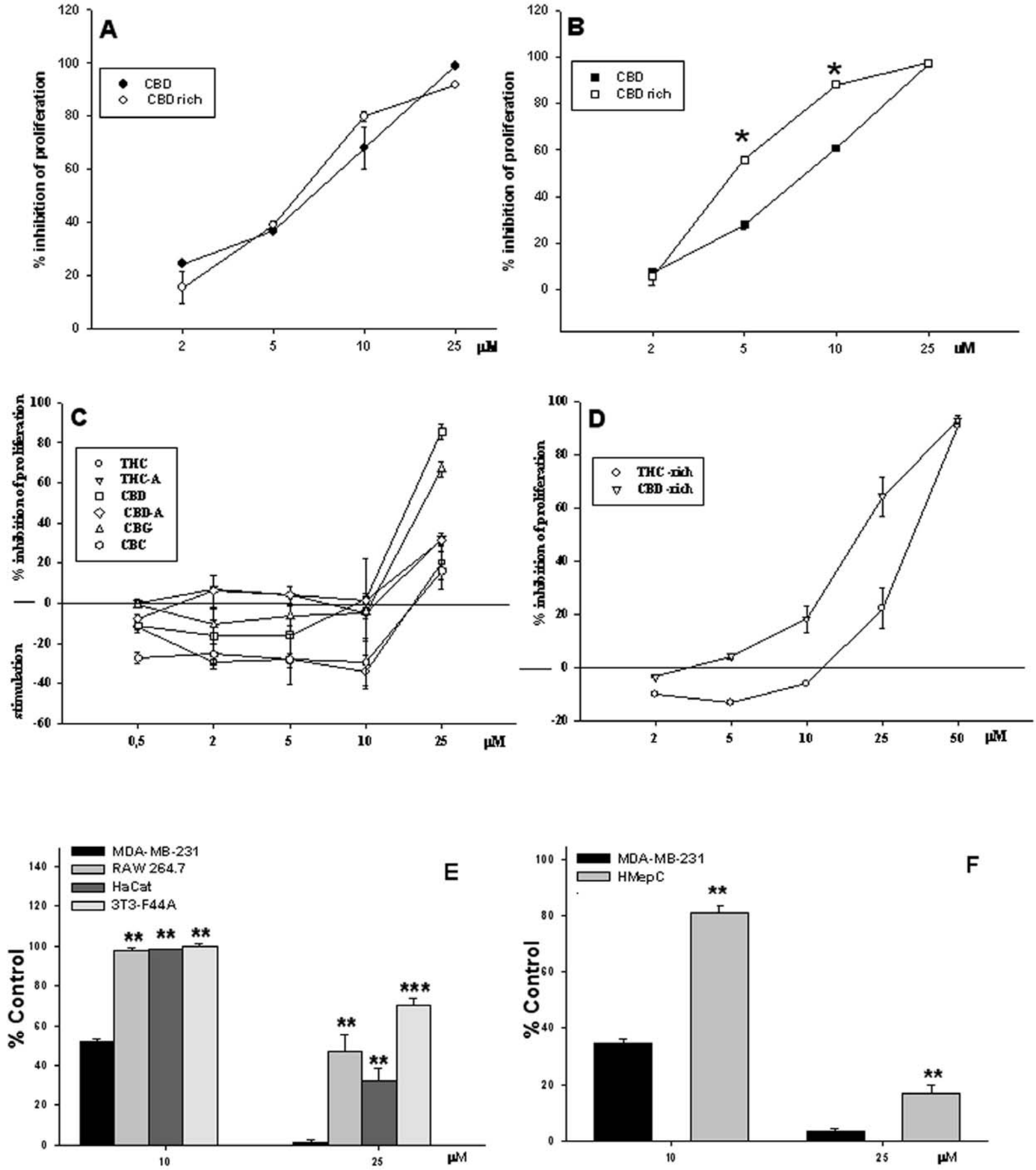
A
CBD
CBD rich
% inhibition of proliferation
μM
B
CBD
CBD rich
% inhibition of proliferation
μM
C
THC
THC-A
CBD
CBD-A
CBG
CBC
% inhibition of proliferation
stimulation
μM
D
THC -rich
CBD -rich
% inhibition of proliferation
μM
E
MDA-MB-231
RAW 264.7
HaCat
3T3-F44A
% Control
μM
F
MDA-MB-231
HMepC
% Control
μM

Figure 3

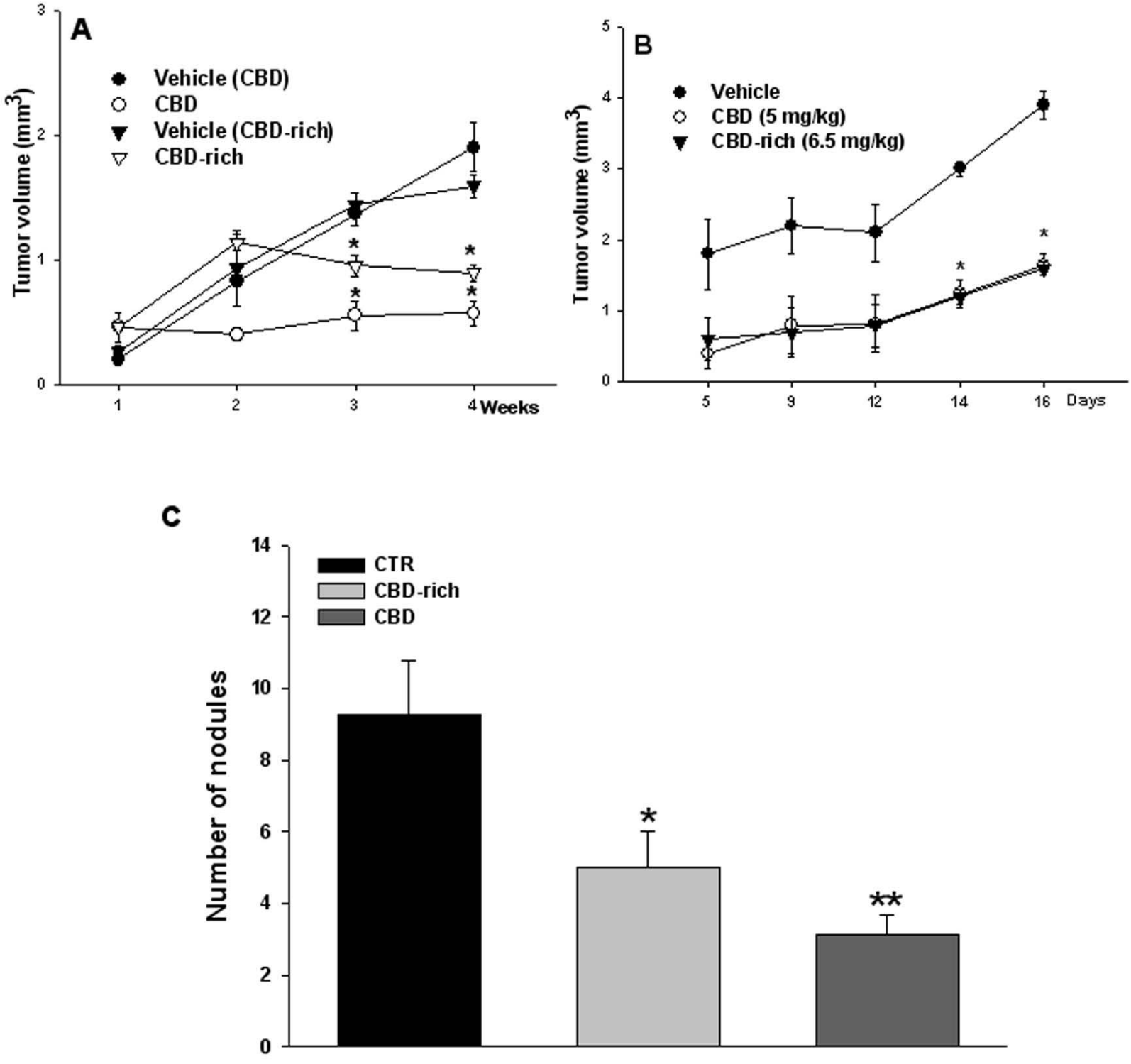
A
Vehicle (CBD)
CBD
Vehicle (CBD-rich)
CBD-rich
Tumor volume (mm3)
Weeks
B
Vehicle
CBD (5 mg/kg)
CBD-rich (6.5 mg/kg)
Tumor volume (mm3)
Days
C
CTR
CBD-rich
CBD
Number of nodules

Figure 4

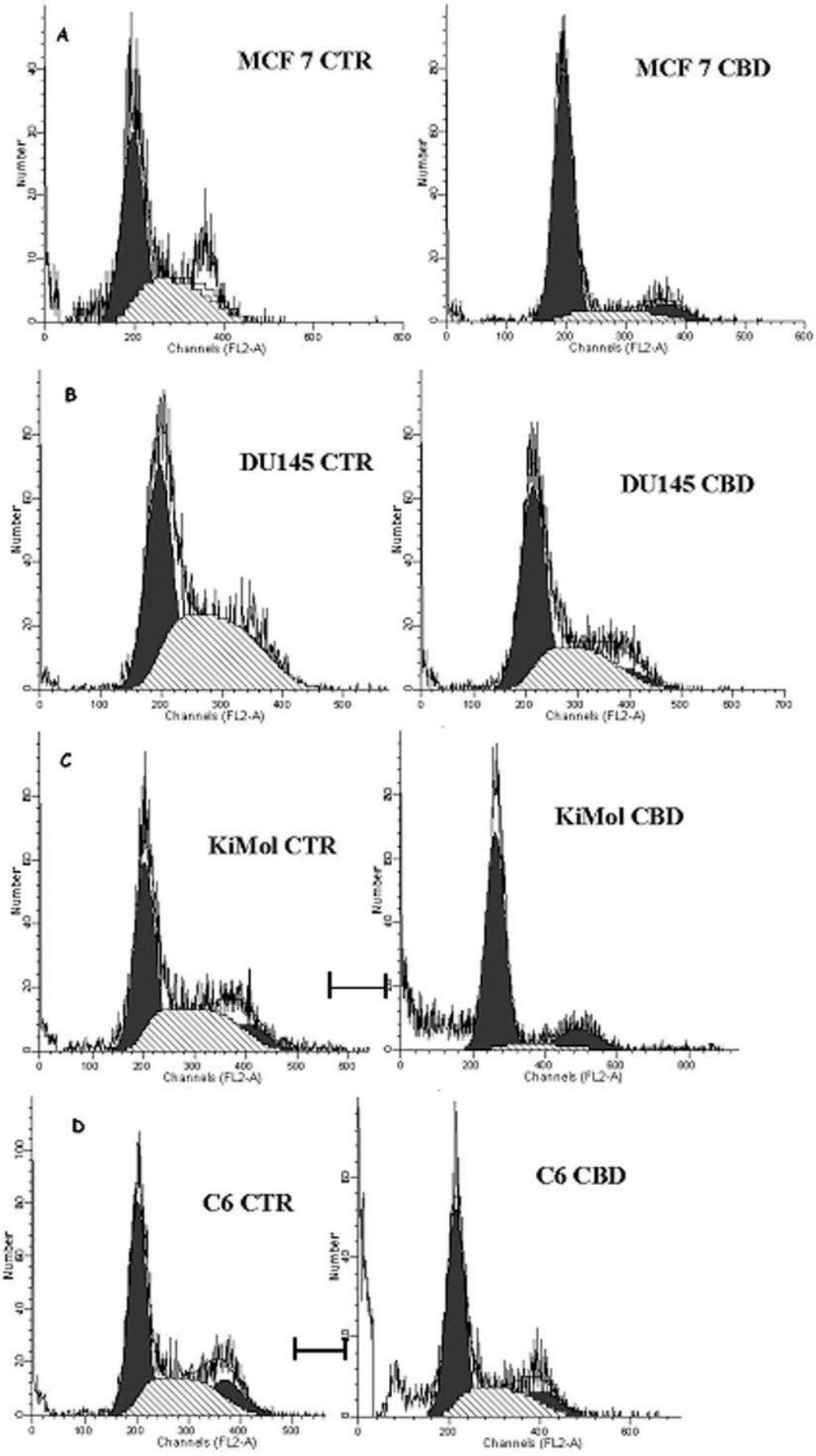
A
MCF 7 CTR
MCF 7 CBD
B
DU145 CTR
DU145 CBD
C
KiMol CTR
KiMol CBD
D
C6 CTR
C6 CBD
Number
Channels (FL2-A)

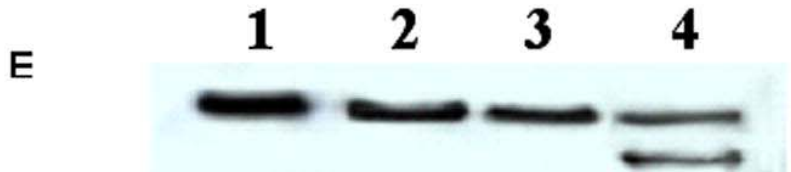
E
1
2
3
4

Figure 5

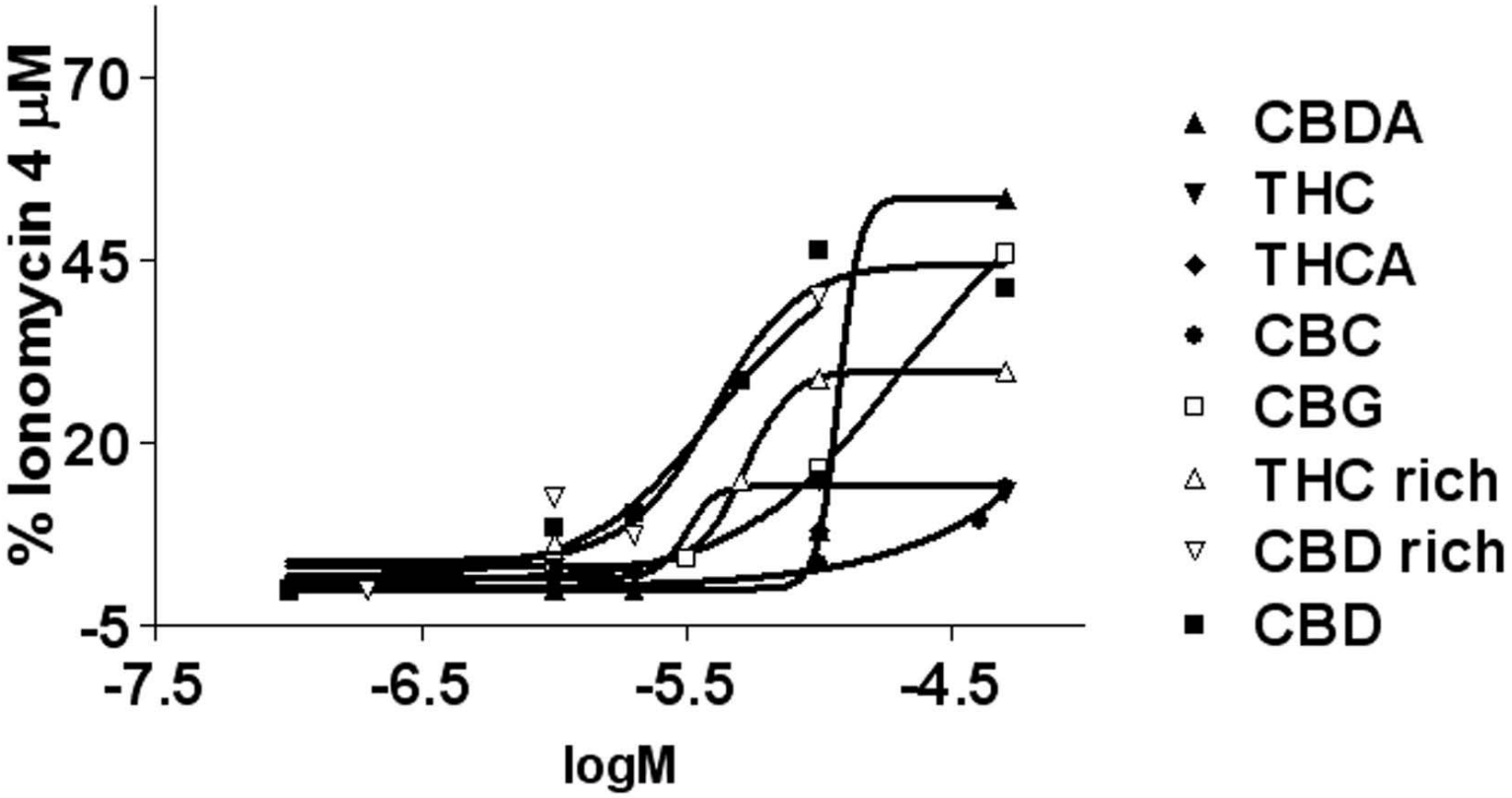
% Ionomycin 4 μM
70
45
20
-5
-7.5
-6.5
-5.5
-4.5
logM
CBDA
THC
THCA
CBC
CBG
THC rich
CBD rich
CBD

Figure 6

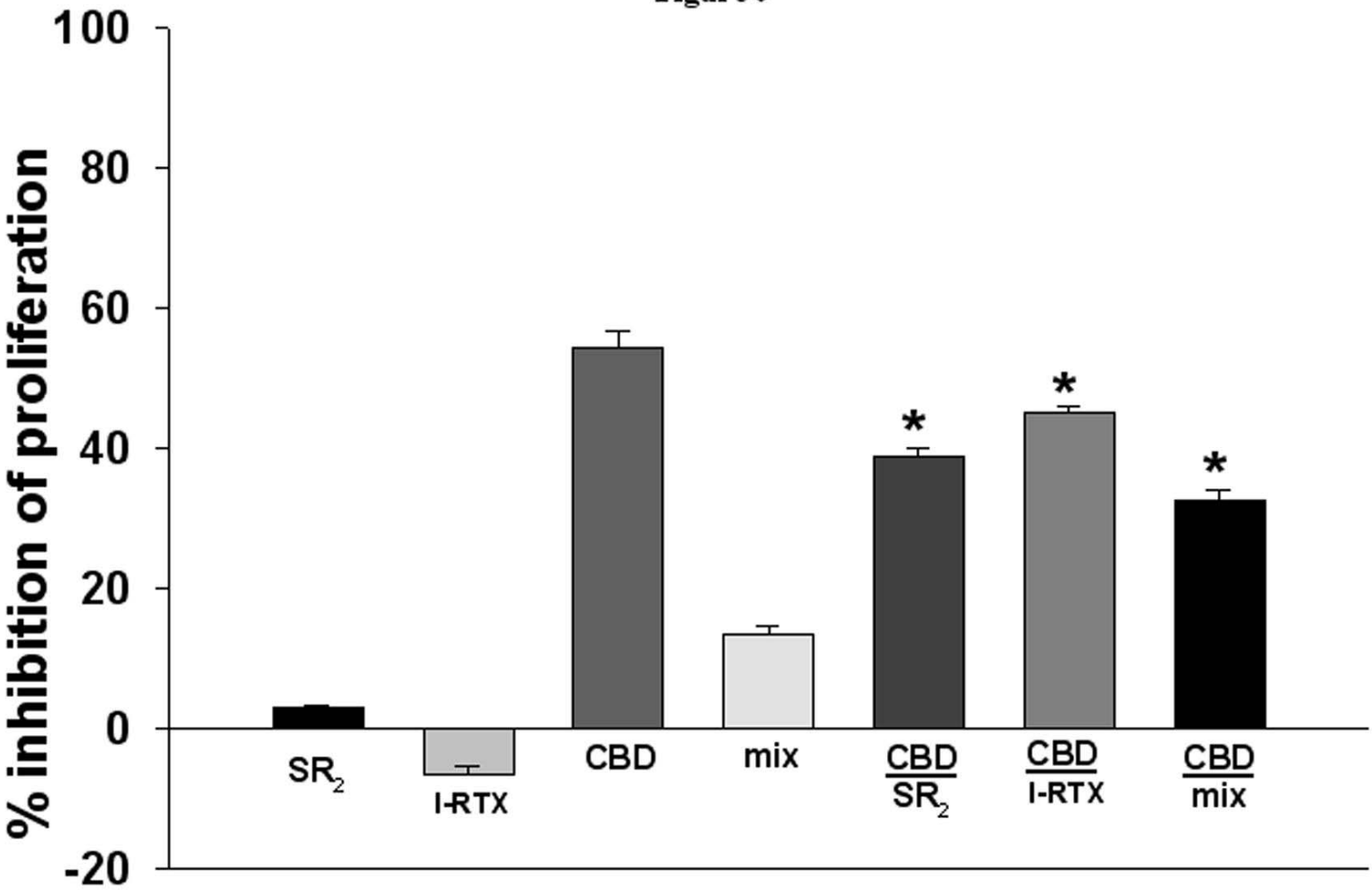
100
80
60
40
20
0
-20
% inhibition of proliferation
SR2
I-RTX
CBD
mix
CBD / SR2
CBD / I-RTX
CBD / mix
*
*
*

Figure 7

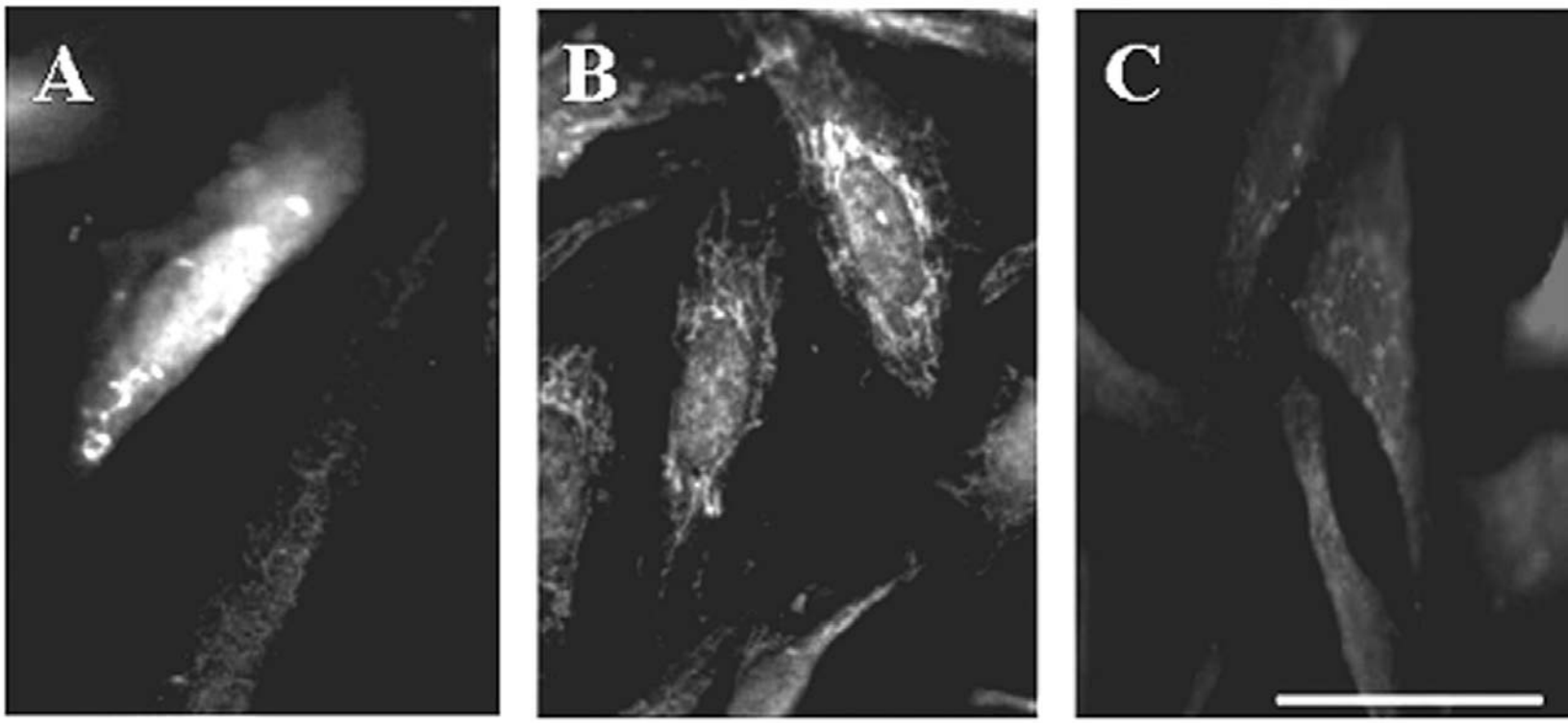

Figure 8

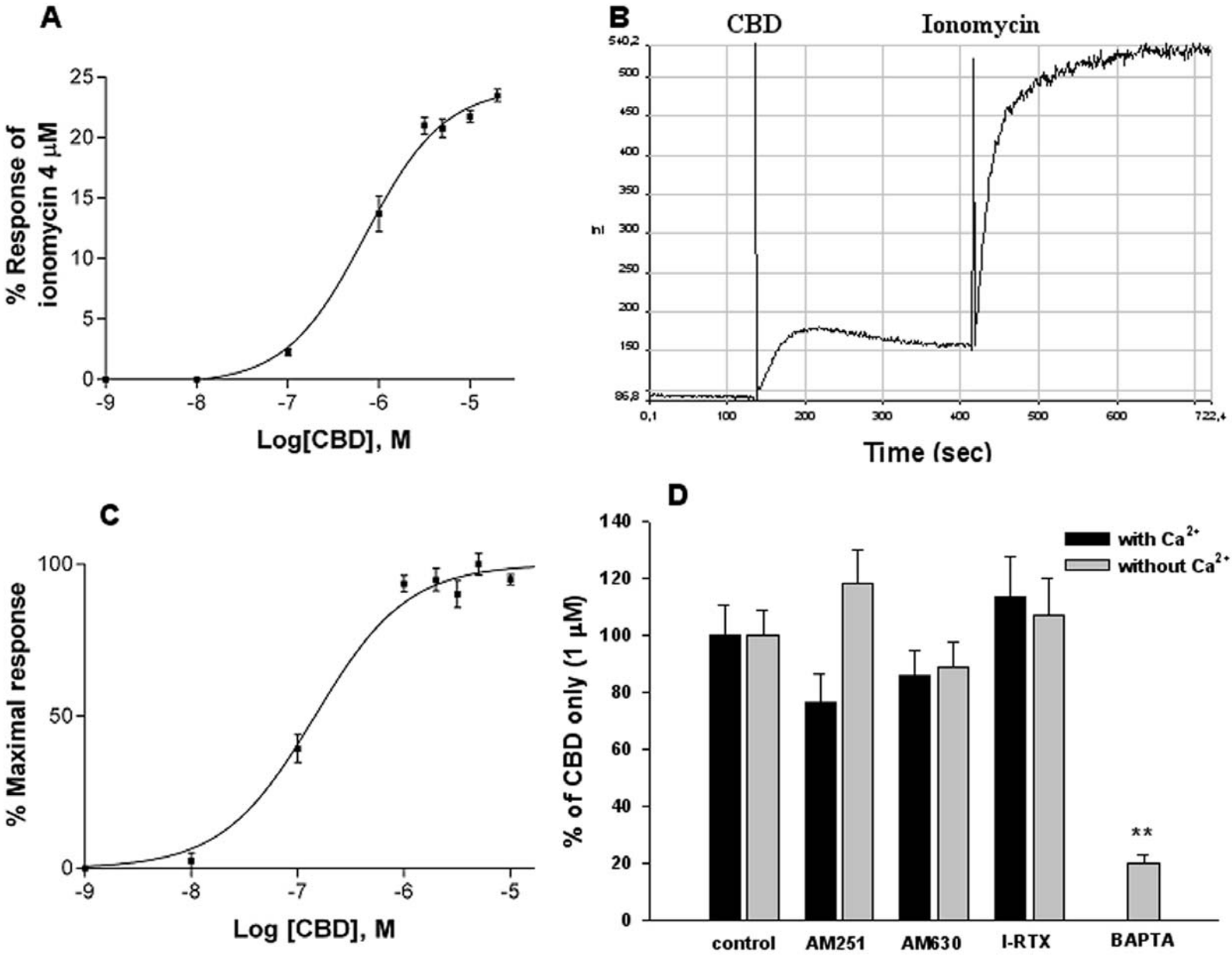
A
% Response of ionomycin 4 μM
25
20
15
10
5
0
-9
-8
-7
-6
-5
Log[CBD], M
B
CBD
Ionomycin
540,2
500
450
400
350
300
250
200
150
86,8
nl
0,1
100
200
300
400
500
600
722,4
Time (sec)
C
% Maximal response
100
50
0
-9
-8
-7
-6
-5
Log [CBD], M
D
% of CBD only (1 μM)
140
120
100
80
60
40
20
0
with Ca2+
without Ca2+
**
control
AM251
AM630
I-RTX
BAPTA

Figure 9

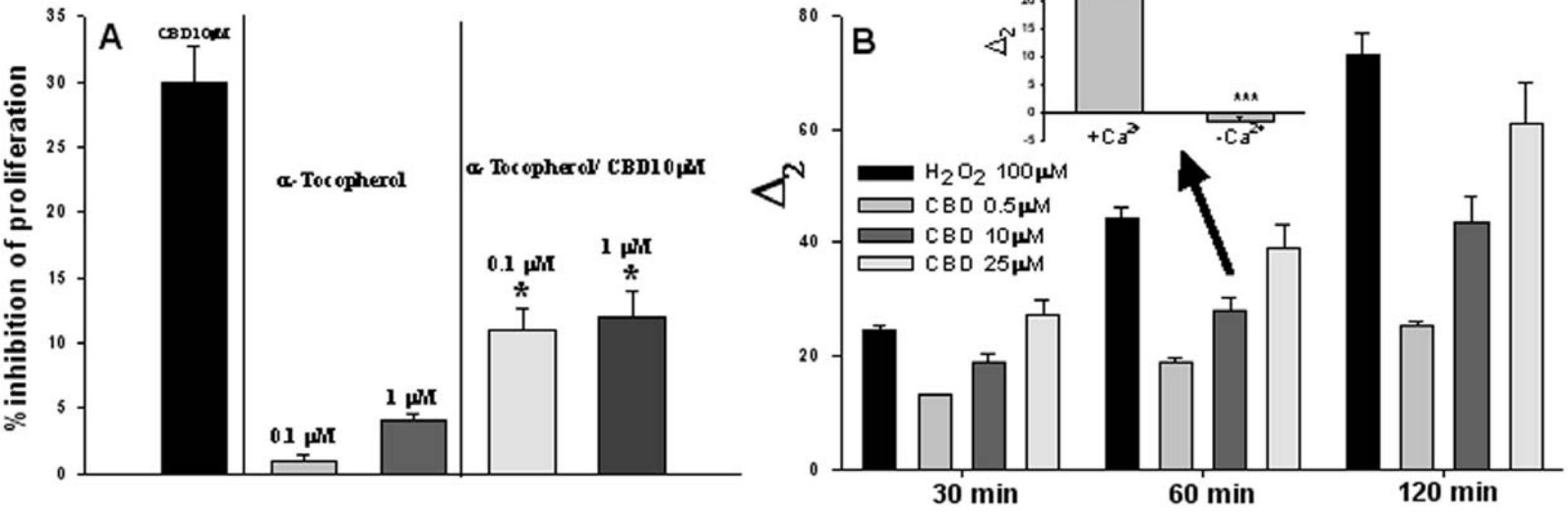
A
CBD10μM
α-Tocopherol
α-Tocopherol/ CBD10μM
0.1 μM
1 μM
0.1 μM
1 μM
% inhibition of proliferation
B
Δ_2
H_2O_2 100μM
CBD 0.5μM
CBD 10μM
CBD 25μM
+Ca
-Ca
AAA
30 min
60 min
120 min

Figure 10

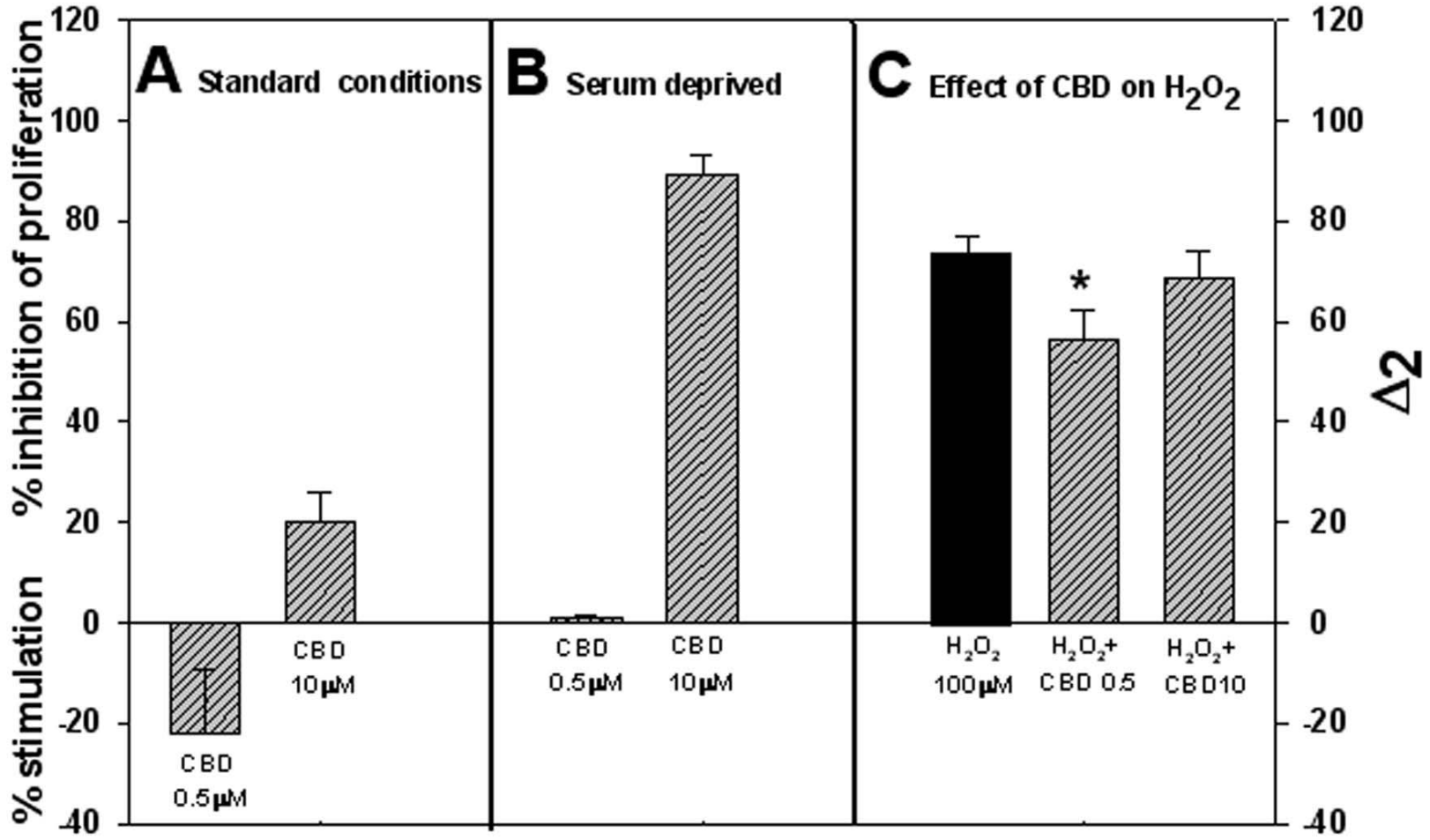
A Standard conditions
B Serum deprived
C Effect of CBD on H_2O_2
% stimulation
% inhibition of proliferation
120
100
80
60
40
20
0
-20
-40
CBD 0.5µM
CBD 10µM
CBD 0.5µM
CBD 10µM
H_2O_2 100µM
H_2O_2+ CBD 0.5
H_2O_2+ CBD10
*
Δ2